DOE/NASA/0086-79/1
NASA CR 159695
ETI 1279

(NASA-CR-159695) STUDY OF ADVANCED RADIAL OUTFLOW TURBINE FOR SOLAR STEAM RANKINE ENGINES (Energy Technology, Inc., Cleveland, Ohio.) 74 p HC A04/MF A01 CSCL 10B
N80-16483
Unclas
G3/44 11943

STUDY OF ADVANCED RADIAL OUTFLOW TURBINE FOR SOLAR STEAM RANKINE ENGINES

CECIL MARTIN
TERRY KOLENC
ENERGY TECHNOLOGY INCORPORATED

FEB 1980
RECEIVED
NASA STI FACILITY
ACCESS DEPT.

DECEMBER 1979

PREPARED FOR
NATIONAL AERONAUTICS AND SPACE ADMINISTRATION
LEWIS RESEARCH CENTER
UNDER CONTRACT DEN 3-86

FOR
U.S. DEPARTMENT OF ENERGY
ENERGY TECHNOLOGY OFFICE
CENTRAL SOLAR TECHNOLOGY DIVISION

FOREWARD

The work described herein was conducted by Energy Technology Incorporated under NASA Contract DEN3-86. Project funding was provided by the Department of Energy (DOE) Advanced Solar Technology Division. The DOE Program Manager was Martin Gutstein. Robert Hyland, of the NASA Lewis Research Center, served as the Contract Manager for NASA, and Terry Kolenc was the Project Manager for ETI.

TABLE OF CONTENTS

SECTION PAGE

Summary 1

Introduction 2

Concept of Radial Outflow Turbine 3

Turbine Analysis 4

- Assumptions (re, Blade Angle, Tip Speed, etc.) 4
- Efficiency -- Last Stage 5
- Turbine Efficiency (Dry) 6
- Turbine Efficiency (Wet) 7
- Shaft Speed Limitations 8
- Turbine Efficiency as a Function of Number of Stages 9

Steam Rankine Cycle Parametrical Analysis Effect of Reheat 13

- Effect of Reheat 14
- Effect of Feedwater Heating 14
- Minimizing Configurations Over Power Range 16

Power Conversion Subsystem Efficiency 18

- Gearbox and Generator 18
- Boiler Feed Pump 18
- Condenser 18
- Auxiliaries 19
- Power Conversion System Efficiency 20
- Part Load Operation and Performance 20

Controls 23

- Engine Controls 23
- System Control and Power Output 24

Conclusions 26

Symbols 28

Figures 30

References 69

LIST OF FIGURES

FIGURE	TITLE	PAGE
1	Radial Outflow Turbine	30
2	ETI Turbine/Gearbox Layout	31
3	Turbine Single Stage Performance References	32
4	Turbine Efficiency vs. Reynolds Number	33
5	Overall Turbine Efficiency vs. Last Stage Efficiency and Number of Stages	34
6	Last Stage Efficiency/Turbine Efficiency, (Z Factor)	35
7	Ideal Turbine Expansion	36
8	Examples of Turbine Moisture in Utility Powerplant Expansion	37
9	Gearbox Shaft Speed vs. Power Level	38
10	Turbine Shaft Speed vs. Power Output	39
11	Turbine Efficiency vs. Number of Stages	40
12	Steam Rankine Engine Performances vs. Number of Turbine Stages	41
13	Basic Steam Rankine Cycle	42
14	Steam Rankine Cycle Calculation Sheet	43
15	Actual Turbine Expansion	44
16	Steam Rankine (Basic) Engine Performance vs. Temp/Press/Power Output	45
17	Steam Rankine (Basic) Engine Performance vs. Temp/Press/Power Output	46
18	Steam Rankine (Basic) Engine Performance vs. Temp/Press/Power	47
19	Steam Rankine (Basic) Engine Performance vs. Temp/Press/Power	48
20	Steam Rankine (Basic) Engine Performance vs. Temp/Press/Power	49
21	Reheated Steam Rankine Cycle	50

FIGURE	TITLE	PAGE
22	Reheated Steam Rankine Cycle Calculation Sheet	51
23	Comparison of Reheated & Basic Rankine Cycle Performance	52
24	Steam Rankine Cycle With Feedwater Heating	53
25	Steam Rankine Engine With Feedwater Heating	54
26	Feedwater Heating Steam Rankine Cycle Calculation Sheet	55
27	Actual Turbine Expansion With Extraction For Feedwater Heating	56
28	Steam Rankine Performance With Feedwater Heating	57
29	Turbine Family Concept	58
30	Gearbox and Generator Efficiency vs. Power Output	59
31	Steam Rankine Engine Efficiency Calculation Sheet	60
32	Engine Efficiency vs. Turbine Inlet Temperature & Power Output	61
33	Engine Efficiency vs. Turbine Temperature & Power Output	62
34	Gearbox Part Load Performance	63
35	Turbine Part Load Performance	64
36	Rankine Engine Part Load Performance	65
37	Steam Rankine Engine Part Load Performance vs. Power Output	66
38	Power Conversion Subsystem and Plant Performance vs. Load	67
39	Solar Insolation Model	68

SUMMARY

An analytical investigation was conducted to determine the performance characteristics of various steam Rankine engine configurations for solar electric power generation. The analysis was based upon an advanced steam turbine developed by Energy Technology Inc. The range of interest for the study was defined by limiting the following parameters:

Turbine Inlet Temperature: 600°F to 1300°F
Turbine Inlet Pressure: 400 PSIA to 2000 PSIA
Condensing Temperature: 65°F to 130°F
Power Output: 100 KW to 5000 KW.

The engine configurations analyzed resulted in Rankine cycle efficiencies from 25 percent to 44 percent not including losses.

The effects of rotating equipment losses and auxiliary power requirements were analyzed to obtain engine efficiencies for a complete power conversion subsystem. Within the range of interest, the above losses resulted in engine efficiencies 9 to 17 percent less than the computed cycle efficiencies.

Off design engine efficiency was studied based on component part load performance. Engine part load efficiency was found to decline uniformly until approximately 20 percent of full load, where the rate of decrease of engine efficiency increased significantly.

ETI's steam turbine was investigated to determine: (1) a method for predicting performance from experimental data, (2) the flexibility of a single design with regard to power output and pressure ratio, and (3) the effect of varying the number of turbine stages. All turbine designs were restricted to be compatible with commercially available gearboxes and generators.

Several operating methods and control schemes for the steam Rankine engine were investigated. From an efficiency and control simplicity standpoint, the best approach was: (1) hold turbine inlet temperature constant, (2) vary turbine inlet pressure to match load, and (3) allow condenser temperature to float maintaining constant heat rejection load.

INTRODUCTION

With our nation's interest in switching to renewable energy sources, the Department of Energy has been pursuing the generation of electric power from solar energy. It has been found that an engine with a high conversion efficiency of thermal to electric power is required to make this concept economically viable. To produce the level of efficiency required with a steam Rankine engine, a high temperature, high pressure cycle and a high efficiency, low cost expander is needed.

Since 1972, Energy Technology Inc. has worked on the development of an advanced, small (under 5000 KW) steam turbine. The objective of the R&D effort has been to provide, at low cost, characteristics not available in commercial small steam turbines; these being the capability to: (1) accommodate inlet temperatures to 1300°F, (2) provide high efficiency throughout the complete load range for applications with pressure ratios greater than 40 to 1, and (3) accommodate extraction ports for feedwater heating. Because of these characteristics, ETI's turbine was ideally suited for solar electric power generation and thus became the basis for this study.

The investigation was directed towards modeling the performance of a turbine driven, steam Rankine power conversion subsystem to provide useful information for solar electric power system designers. A highly simplified design procedure for the turbine was built upon experimental data and previous design experience. This was done to permit the large number of Rankine cycles within the study's wide range of interest to be analyzed on a desktop computer.

A sufficient number of Rankine cycles were evaluated to permit cycle efficiency to be obtained for any combination of the four basic parameters, which were the following:

Turbine Inlet Temperature
Turbine Inlet Pressure
Condensing Temperature
Power Output.

A limited number of Rankine cycles was evaluated to show representative results for:

Reheated Cycles
Feedwater Heating Cycles
Off Design Performance
Overall Engine Efficiency
Effect of No. of Turbine Stages.

CONCEPT OF THE RADIAL OUTFLOW TURBINE

The basic geometry of the radial outflow (ROF) turbine under development at ETI is shown in Figure 1. The turbine is a multistage design, with each stage composed of one stationary and one rotating blade row. The working fluid, steam, in the case of this study, enters the turbine at the center of the fixed stator. The fluid then expands radially outward through alternating, concentric stator and rotor blade rows, where its enthalpy drop is converted to shaft power by the rotating blade rows. The ROF turbine geometry has several advantageous characteristics as follows:

1. In most cases, only a single rotor disc is required to carry the required number of blade rows. This produces a lightweight rotor permitting an overhung rotor arrangement, reducing bearing and seal requirements.

2. Due to the compact arrangement, described above, thermal losses are minimized.

3. Because the flow is radial, the turbine blades have a constant untwisted profile along their length. High precision blades can therefore be obtained from low cost manufacturing methods, and a simple and accurate aerodynamic analysis can be used for the design.

4. In most cases, full admission can be used on all stages due to the radial arrangement which puts the low volumetric flow stages at a small diameter.

5. With almost negligible change to the turbine housing, the power output of a given unit can be adjusted by changing the turbine blade heights by a proportionate amount. The ability to do this is discussed in more detail later.

6. Because of the simplicity of the assembly, tight tolerances and thus small clearances between the rotor and stator can be easily maintained. This minimizes leakages of the working fluid in the turbine--one of the principal losses of expander efficiency.

A typical turbine/gearbox with an overhung rotor arrangement is shown in Figure 2. The nine stage turbine and single reduction gearbox shown is representative of the units contained in this study. The rolling element bearings shown, however, are not typical of 100 KW--5 MW gearboxes; most use journal bearings. The electric generator will have its own bearing system.

TURBINE ANALYSIS

A method for estimating the efficiency for ETI's radial outflow (ROF) turbine design was needed to be able to evaluate overall power conversion subsystem performance. Within the program's work scope, it was not possible to do a detailed turbine design for all the parametric Rankine engine combinations. Therefore, a scheme was devised which would give a good rough approximation of the expected turbine performance.

A decision was made to use the turbine's last stage as a basis and to compute the performance of that stage utilizing the design experience and test data of ETI and others. Reynolds number was selected as the best indicator of stage efficiency. In a multi-stage turbine, the energy release per stage generally increases from inlet to exit. As a result, the last stage has the greatest effect on the turbine's overall performance.

The four sections that follow describe the procedure developed for estimating the efficiency of ETI's radial outflow turbine.

ASSUMPTIONS (Re, BLADE ANGLE, TIP SPEED, ETC.)

Reynolds number is a dimensionless parameter commonly used to correlate turbine performance. Experimental efficiency vs. Re data was collected to be used as a basis for the turbine calculations. Sources containing data defining the current state of the art in small turbomachinery were selected from this reference pool. This data is listed in Figure 3. Much of this information was obtained from experimental work conducted at the NASA-Lewis Research Center. The references of Figure 3 define Re with the following equation:

$$Re = \frac{m}{\mu r_t}$$

This is different from the classical definition of Re, which is usually specified as follows:

$$Re = \frac{\nu D_h}{K}$$

The hydraulic diameter (D_h) being defined as:

$$D_h = \frac{4A}{W}$$

By using the continuity equation ($m = \rho VA$), the definition of hydraulic diameter from the first Re equation can be separated out, yielding:

$$D_h = \frac{A}{r_t}$$

Due to the difficulty of translating all of the reference data, a decision was made to utilize the Re definition based on the turbine tip radius (r_t), rather than the conventional one based on the wetted perimeter (W) of the flow area.

To maintain relative simplicity in the turbine efficiency calculation procedure, some assumptions were made regarding the radial outflow turbine geometry. These resulted in compromises on the optimum turbine efficiency, but produced results of sufficient accuracy for the objectives of the study. These assumptions are summarized as follows:

1. A blade exit angle of 18° was used. ETI has constructed blade rows with exit angles less than 18°, but due to the high exit volumetric flow rates associated with many of the cycles within the range of interest, the above value was specified.
2. The last stage tip speed was specified as 90 percent of the spouting velocity. This compromise was necessitated by the fact that the majority of the turbines investigated would be exhausting wet steam.
3. A ratio of the turbine rotor tip radius to the last stage rotor blade height of 11.5 was specified. This was an average value taken from past radial outflow design experience. The ratio is related to the rotor's mechanical design.

Substitution of these values into the Re equation produces this result:

$$Re = 2.59 \frac{b^2 N}{K}$$

The turbine rotor last stage exit blade height (b) can be defined using the continuity equation as follows:

$$b = \frac{m \; ve \; N}{60060 \; (V_{sp})^2}$$

Turbine shaft speed (N) selection is discussed in detail in a later section. It is based on these factors:

1. Available commercial gearboxes and generators.
2. Turbine mechanical design limits.

EFFICIENCY--LAST STAGE

Turbine state-of-the-art performance, listed in Figure 3, is shown plotted as a function of Reynolds number in Figure 4. The data of Figure 4 is for single stage subsonic flow turbines of both radial and axial flow configurations. The fact that all the turbines of this correlation are subsonic is significant. For solar electric power generation, a multi-stage, subsonic flow turbine is needed to: (1) accommodate the high design pressure ratios, and (2) deliver good part load efficiency. The aerodynamics of radial and axial flow turbine configurations differ only in that three dimensional blades are needed in the axial turbine to handle the centrifugal effect.

A best fit curve was drawn through the data of Figure 4. Also on this graph, points were plotted which represent the last stage of several ETI radial outflow turbines. The ETI turbines show a slight improvement over the previous state of the art. This is primarily the result of the development of manufacturing techniques to produce more accurate blade profiles and the use of proportionately smaller blade tip clearances. A curve representing the last stage performance of ETI's radial outflow turbine was drawn on Figure 4--parallel to the state-of-the-art curve. The equation of the curve which determines the last stage efficiency is as follows:

$$\eta_1 = 0.650 \ Re^{0.0266}$$

TURBINE EFFICIENCY (DRY)

To estimate overall turbine efficiency from the last stage efficiency, two principal factors must be accounted for:

1. The number of stages.
2. The level of moisture in the turbine expansion.

Turbine performance, as a function of the number of stages for a fixed pressure ratio, is discussed in a later section. Near optimum performance in a subsonic, multi-stage design occurs at a stage pressure ratio (inlet pressure divided by exit pressure) of approximately a value of two. Based upon this assumption, an equation for the number of stages in a given turbine design was written:

$$x = 1.4 \ln (P_i/P_e)$$

In the above equation, X is always rounded to the nearest integer.

Several attempts were made to develop an equation for overall (dry) turbine efficiency as a function of last stage efficiency and the number of stages. No satisfactory solutions could be obtained, nor were any available in ETI's library of turbine design references. The design of a multi-stage turbine is relatively complex. The overall efficiency is greater than a weighted (by power output) average of the stage efficiencies, because of the reheat effect from the mixing of the leakage flow.

The ratio of the overall (dry) turbine efficiency divided by the turbine's last stage efficiency was designated as the "Z" factor. For a single stage turbine, it is obvious that the Z factor is equal to a value of one. For the multi-stage designs of this study, other Z factors were determined empirically using a graphical method.

A schematic drawing showing the radial outflow (ROF) turbine geometry appears in Figure 1. The Z factors associated with several detailed ROF turbines are shown plotted in Figure 5. The data used to compute these factors is included in Figure 6. The shape of the curve is uniquely associated to the characteristics of the ROF turbine. As stages are added to the single stage design, the Z factor decreases. This is because the additional stages are forced to operate at non-optimum u/c ratios--due to reduced tip speeds imposed on the inner stages of the ROF geometry. For turbines of five or more stages, the Z factor increases. This results from two ROF turbine characteristics stated earlier: (1) individual stages in an ROF design increase in efficiency from inlet to exit due to improved blade jet (u/c) velocity ratios at the larger diameters, and (2) the energy release per stage increases from inlet to exit.

In summary, the overall dry expansion efficiency is defined as:

$$\eta_d = Z\ [0.650\ Re^{0.0266}]$$

Where Z is obtained from Figure 5 and Re is defined by the following equation:

$$Re = 2.59\ \frac{b^2 N}{K}$$

with,

$$b = \frac{m\ \nu e\ N}{60060\ (V_{sp})^2}\ ;$$

$$m = \frac{3412\ E}{(\Delta h_i)\ (\eta_w)}\ ;$$

$$N = 141957\ (E)^{-0.2947} - 6533$$

(See Figure 10)

An ideal turbine expansion enthalpy drop (Δh_i) is shown plotted on a Mollier Chart in Figure 7. Design specifications for this steam Rankine cycle being as follows:

Turbine Inlet Temperature: 1100°F
Turbine Inlet Pressure: 1000 psia
Condenser Pressure: 1.0 psia

The computing of m from Δh_i is a reiterative process, which is described in the section on Steam Rankine Cycle Performance.

TURBINE EFFICIENCY (WET)

Overall turbine efficiency (η_d) must be adjusted whenever the quality of the turbine's exhaust steam is less than a value of one. The equation correcting for moisture in a turbine expansion is a modified Baumann rule, as follows:

$$\eta_w = \eta_d \, [1 - \alpha \, (1-Q) \, (\Delta h_w/\Delta h_t)]$$

The principal parameters being: (1) the Baumann factor [$\alpha = 0.35$] which is discussed in Reference 3, (2) the exhaust steam quality (Q), and (3) the fraction of the turbine expansion in the saturated vapor region [$\Delta h_w/\Delta h_t$].

The operating life of the turbine is strongly linked to the moisture in the expansion. Utility powerplant practice, examples of which are shown in Figure 8, has been to limit turbine exhaust moisture to maintain turbine blade erosion rates consistent with design life in the 20-30 year range.

All of the turbines shown in Figure 8 are of an axial flow configuration. With this type of turbine geometry, the centrifugal force from the shaft rotation causes moisture droplets to collect near the blade tips. To counteract this problem, axial flow turbines operating with high exhaust moisture have ports in the blade shrouds to extract the moisture. With the radial outflow configuration, the centrifugal force field is in the direction of the expansion. As a result, moisture droplets are not as easily formed in the ROF turbine, and highe moisture levels can be tolerated before blade erosion becomes significant.

In order to have ROF turbine designs consistent with a minimum 20-year design life, turbine exhaust moisture was restricted to a maximum of 15 percent for the steam Rankine cycles investigated. All charts showing Rankine cycle performance have an 85 percent turbine exhaust quality line, which limits the cycle parameter combinations that can be specified.

SHAFT SPEED LIMITATIONS

Within the 100 KW to 5 MW power range of the study, the maximum generator speed readily available in commercial units is 1800 rpm, for most manufacturers, 100 KW was the cutoff point for 3600 rpm generators. As a result, turbine shaft speed is limited by the available gear ratio and pinion speeds from the gearbox suppliers. A survey of these parameters as a function of power level produced the data shown in Figure 9. Gear manufacturers are limited by the smallest diameter shaft that can be cut and the maximum pitch line velocity. For these reasons, few low power, high speed gearboxes are available.

A best fit curve was drawn through the data of Figure 9. This curve, shown in Figure 10, was used to define turbine shaft speed (N) as a function of power level (E). An equation for this curve was determined to be the following:

$$N = 141957 \, (E)^{-0.2947} - 6533$$

In most cases, the above equation is used to specify the turbine shaft speed, except when turbine stress limitations would be exceeded. In the ROF turbine design, the limiting factor is the bending stress on the blades of the last turbine rotor stage.

This stress can be approximated by the following equation:

$$S = 0.01625\ N\ V_{tip}b$$

The rotor tip speed (V_{tip}) can be approximated by substituting the spouting velocity (V_{sp}) from the turbine performance calculations. The blade height (b) in the above equation is computed from the equation given in the section on Turbine Efficiency vs. Reynolds Number. Generally, the stress equation will become the controlling factor whenever the volumetric flow rate of the steam at the exit of the turbine becomes very large. This occurs at low condensing temperatures and/or very high power output.

It should be noted that the above stress equation is applicable only to ETI's turbine design. Radial outflow turbines built by other manufacturers are not likely to possess the tip speed capability which has been engineered into ETI's design. Other ROF turbine builders generally utilize counter-rotating turbine blade rows to achieve comparable relative tip speeds. This is a much more costly approach and one of the main reasons why this type of turbine design has not seen very wide application in this country.

TURBINE EFFICIENCY AS A FUNCTION OF NUMBER OF STAGES

Turbine efficiency can be related to four basic overall parameters:

1. Blade jet speed ratio
2. Speed-work parameter
3. Specific diameter
4. Specific speed.

Where a particular type of velocity diagram is used, as dictated by the turbine geometry selected, only one of the above parameters is needed to correlate efficiency. This is discussed in Reference 1.

The speed-work parameter was selected to analyze the effect of varying the number of stages in a fixed pressure ratio design. The speed-work parameter (λ) of an individual stage is defined as:

$$\lambda = \frac{\mu^2}{gJ\Delta h}$$

Optimum stage performance occurs when $\lambda = 1$.

The overall speed-work parameter ($\bar{\lambda}$) for the completion turbine is defined as:

$$\bar{\lambda} = \frac{\mu^2}{gJ\Delta h_t}$$

Figure 11 shows overall total-to-static turbine efficiency as a function of the overall speed-work parameter and the number of turbine stages. Figure 11, which is reproduced from Reference 1, was used as the basis for study of the effect of the number of turbine stages on Rankine cycle performance.

A family of Rankine cycles having a power output of 1000 KW and a condensing temperature of 110°F was chosen for a sample. Rankine cycle efficiency as a function of turbine inlet conditions and the number of turbine stages is shown in Figure 12. For each of the three inlet pressures of Figure 12, the highest number of stages shown corresponds with the number used for the basic Rankine cycle calculations discussed earlier. For each reduction in the number of stages, cycle efficiency decreases between 1.5 and 3.0 percent. In a 1000 KW solar-electric plant, each percentage point change in cycle efficiency could result in a difference of $60,000 in solar receiver cost. (This is based on data from Reference 4.) The total cost of a 1000 KW, 10-stage turbine is approximately $300,000 for prototype units; production units would be significantly lower in cost. The cost of the turbine is not linearly related to the number of stages. A single stage, 1000 KW turbine would cost nearly $200,000. It is easily seen that reducing the number of stages in the turbine has a pronounced negative effect on overall system cost.

With the radial outflow turbine geometry, there is a limit to the number of stages that can be specified for a single rotor disc design. The mechanical design of the rotor limits tip speeds to values of 1500 ft/sec or less depending on turbine exhaust steam conditions. To obtain a larger diameter disc, permitting more stages to be mounted, the shaft speed must be lowered. It has been ETI's experience that to obtain optimum turbine performance, the highest shaft speed possible should be utilized at a given power level. Otherwise, design of high efficiency inner stages becomes difficult.

The rough turbine designs computed for the basic Rankine cycle calculations were reviewed regarding their adaptability to various condenser pressures. Specifically, the effect of adding or removing a stage at the exit of a particular turbine design was studied.

The final stages of a multi-stage radial outflow turbine have pressure ratios of approximately 2.3 to 1 for optimum performance. Holding shaft speed constant, the addition of another stage at the turbine exit would cause the turbine blade stress to nearly double (using the equation defined previously). For the majority of turbines within the parametric bounds of this study, an additional stage would put the stress beyond the design limit.

Another problem with adding a stage to the exit is that the spouting velocity from the added stator blade row would likely be lower than the relative velocity of the rotor--thus prohibiting steam from entering the rotor. This problem results from the relatively low tip speeds of the turbines of this study, which is the result of operating with saturated exhaust steam.

Removing a stage at the exit of the turbine, such as to adapt a water-cooled to an air-cooled condensing design, poses no design problems. The overall turbine efficiency would decrease by about 3 percent, because the turbine's most efficient stage would be deleted. To remove a stage and maintain the same power output, the blade heights of the remaining stages would have to be increased. To accomplish this, mass flow would be increased by 6 to 12 percent. However, blade stress would still be lower than the same power turbine with the lower exhaust pressure.

STEAM RANKINE CYCLE PARAMETRICAL ANALYSIS

The steam Rankine cycle, in its simplest form, consists of these elements:

1. Preheater/boiler
2. Expander
3. Condenser
4. Feed pump.

These elements were designated as "the basic steam Rankine cycle" and are shown on a temperature-entropy (T-S) diagram in Figure 13.

The critical point temperature for steam is 705°F. The temperature range of interest for this solar electric power study is from 600°F to 1300°F. Therefore, another element must be added to the basic cycle--a superheater. This is shown on the T-S diagram in Figure 13. Both diagrams in Figure 13 are shown without the feed pump, which would be nearly invisible if drawn to scale. The power required to drive this pump will be covered later. For now, it will be deleted for simplicity, since it is a relatively insignificant effect, which is not true of some other Rankine cycle working fluids.

The basic steam Rankine cycle was analyzed to be able to compare the relative performance as related to these parameters:

1. Turbine Inlet Temperature (600°F to 1300°F)
2. Turbine Inlet Pressure (400 psia to 2000 psia)
3. Condensing Temperature (65°F to 130°F)
4. Output Power (100 KW to 5 MW).

Shown above is the range of interest for these parameters for steam Rankine driven solar-electric power applications as jointly determined by DOE, NASA and ETI.

A sample cycle efficiency calculation sheet is shown in Figure 14. Each calculation was begun by specifying values for the four parameters named above. Next, values for inlet enthalpy and entropy, and exit enthalpy for an ideal isentropic expansion were obtained from the 1967 ASME Steam Tables. Turbine shaft speed was computed as described in a previous section. Using a reiterative process and the previously derived equations, turbine last stage efficiency was recomputed until the actual turbine exhaust steam conditions matched the estimated values within a tolerance of ± 0.25 percent.

Once the turbine exhaust conditions were established, the last stage blade stress was checked to make sure it was within limits. For the sample calculation of Figure 14, the value was 56,500 psi which was satisfactory. Had this value exceeded the design limit of 70,000 psi, a new, lower turbine shaft speed would have been specified.

Next the Z factor for the conversion from stage efficiency to overall turbine efficiency was obtained from Figure 5. The sample turbine is a nine-stage machine so the Z factor is 0.926. This produced a dry turbine efficiency of 0.877. Finally, the turbine moisture penalty was calculated. The portion of the expansion in the wet region was equal to (137 Btu/lb)/(495 Btu/lb). This was obtained from a plot of the turbine expansion on a Mollier Chart, which is shown in Figure 15. A wet turbine efficiency of 0.869 was calculated as follows:

$$0.869 = 0.877\ [1 - (0.35)\ (1 - 0.904)\ (137/495)]$$

Referring to Figure 13, the heat input to the preheater/boiler/superheater was computed using the mass flow rate of of Figure 14. The power output was a specified value, and the engine's heat rejection is the difference between the heat input and the work output. Cycle efficiency is the work output divided by the heat input.

Cycle efficiency is shown plotted as a function of turbine inlet temperature in Figures 16 through 19. These figures show data for four condensing temperatures, three inlet pressures and three power outputs. By replotting the data of Figures 16 through 19, cycle efficiency as a function of any of the four primary parameters can be obtained. An example of this is Figure 20, which shows cycle efficiency vs. condensing temperature. As was discussed in the section on turbine performance, all the cycle efficiency charts show an 85 percent turbine exit quality line, which is the design limit.

EFFECT OF REHEAT

The basic Rankine cycle of Figure 13 was modified to include a reheater. The reheat cycle is shown on a T-S diagram in Figure 21. Also shown in Figure 21 is a regenerator, which will be discussed later.

A sample reheat cycle calculation sheet is shown in Figure 22. Methods used to compute cycle efficiency are similar to those described for the basic engine in the preceding section. Extraction pressure from the turbine for reheating was defined with the following equation

$$P_x = P_i/(P_i/P_e)^{\frac{1}{2}}$$

This method will roughly balance the work output and moisture content of the two portions of the expansion. After reheating, readmission to the turbine was made at an inlet pressure of 0.97 P . This accounts for the pressure drop in the reheater heat exchanger. Turbine inlet temperature for the second expansion was defined as the original inlet temperature less 50°F. The above specifications should permit low cost heat exchanger design.

Stage efficiency was computed for each of the expansions based on the Reynolds number at the exit of each expansion. The

Z factor for converting from stage efficiency to overall turbine efficiency was selected based on the total number of stages.

In analyzing the reheated cycles, it was found that the use of reheat alone will generally effect a decrease in cycle performance. For the lower inlet temperature cycles under consideration, reheating will change the expansion from partially wet to dry. Thus the turbine efficiency is increased through elimination of the moisture penalty. However, a decrease in turbine performance is simultaneously caused because of the lower Reynolds number from the smaller volumetric flow rate at the turbine exit. The efficiency loss being primarily due to an increase of the relative leakage flow in the turbine. The net result of these two opposing effects was found to be a reduction in turbine performance.

For reheated cycles at the upper end of the temperature range, the turbine exhaust after the second expansion contains a significant amount of residual useful energy. In these cases, a regenerator can be used to recover this energy and utilize it for liquid preheating. A minimum temperature differential of 50°F was specified for the regenerator.

In Figure 23, the change in cycle performance relative to the basic engine is shown. This data is for a 1000 KW turbine output with a 110°F condensing temperature and a turbine exhaust regenerator where applicable. From the graph, the following conclusions can be drawn:

1. Reheating permits the use of lower temperature cycles without exceeding the 85 percent exit quality limit. For example:

INLET PRESSURE (PSIA)	MINIMUM* INLET TEMPERATURE (°F)	
	BASIC CYCLE	REHEAT CYCLE
400	680	--
1000	800	500
2000	1060	700

---

*Based on turbine moisture limitations.

2. Reheating at higher inlet temperatures (above 1000°F) can improve Rankine cycle efficiency up to 12 percent.

EFFECT OF FEEDWATER HEATING

Another modification that can be made to the basic engine is the addition of feedwater heaters for preheating of the boiler inlet fluid. Feedwater heating is shown schematically on a T-S diagram in Figure 24. A portion of the steam flow expanding through the turbine is extracted between stages. This steam is fed to a heat exchanger where it is condensed and subcooled, and finally mixed with the condenser inlet flow. The heat from the condensing steam is transferred to the fluid exiting the condenser.

Multiple extractions can be used depending upon the turbine geometry. Feedwater heating is almost universally used in large steam powerplants to improve cycle efficiency. The technique has not been largely applied to steam engines in the power range of this study due to the fact that commercially available turbomachinery in this power range generally has not been designed to accommodate the extraction ports required.

ETI's ROF turbine is readily adaptable to the addition of steam extraction ports. Individual turbine stage blade heights can be altered to account for the change in mass flow without drastically changing the design. This is not as easily accomplished in an axial flow turbine. The pressures at which steam is available for extraction, however, are restricted by the turbine's configuration, which is dictated by the individual stage pressure ratios. For the purpose of this study, a rough turbine design was worked out for a turbine with a 2,000 psia inlet pressure and a 1.275 psia exhaust pressure. Four potential extraction ports were identified at these pressures: 400, 110, 30, and 7.5 psia. A schematic drawing for a steam Rankine engine with four feedwater heaters is shown in Figure 25.

A sample calculation for a steam cycle with feedwater heating is shown in Figure 26. The enthalpy at the turbine extraction points was determined by using a Mollier Chart. A first trial expansion line was laid out using the specified inlet conditions and exhaust pressure, and an estimated overall turbine efficiency. This process was reiterated until the computed turbine efficiency, including the feedwater extraction flows, matched the estimate within ± 0.25 percent. The enthalpies at the intersection of the appropriate extraction pressure lines were determined. This is shown in Figure 27. The extracted steam was condensed at the extraction pressure and subcooled to within 20°F of the saturation temperature of the succeeding extraction. The subcooled liquid was then mixed with that of the succeeding extraction and subcooled again. This process was continued until the mixed extraction flows had been subcooled to within 20°F of the condensing temperature; then they are mixed with the condenser inlet flow. On the liquid side of the feedwater heaters, the flow is assumed to be at turbine inlet pressure. No allowance for pressure drop in the feedwater heaters, boiler, or superheater was accounted for. In each feedwater heater, the liquid was heated to within 20°F or the temperature of the condensing steam on the vapor side of the heat exchanger.

The mass flow extracted at each port was calculated from this formula:

$$m_e = \frac{h_1 - h_2}{h_3 - h_4} m_i$$

The enthalpy values for the above equation are defined as follows:

h_1 = enthalpy of liquid at feedwater heater exit at temperature = Te - 20°F

h_2 = enthalpy of liquid at feedwater heater inlet at temperature = condenser exit or preceding feedwater heater exit

h_3 = enthalpy of vapor at turbine extraction port

h_4 = enthalpy of liquid at exit of vapor side of feedwater heater at temperature = condensing temperature of succeeding feedwater heater or condenser + 20°F.

Once the extraction flows were determined, the turbine mass flows were computed for each portion of the expansion. With these mass flows and the enthalpies from the Mollier Chart (Figure 27), the turbine work output was computed.

The effect on basic cycle efficiency from the addition of feedwater heating is shown in Figure 28. For this analysis, a power output of 1000 KW and a condenser temperature of 110°F were selected. The results plotted show the effect of using one or more of the available extraction ports (discussed earlier) for the full study range of turbine inlet temperature and pressure conditions. As can be seen, the relative value of using an additional feedwater heater steadily decreases. However, even the last feedwater heater produces almost a 3 percent improvement in cycle efficiency. The cost savings from the reduction in size of the solar receiver should more than offset the cost of even the fourth feedwater heater. A note should also be made of the fact that turbine efficiency decreased by 1 to 5 percent for the cycles analyzed. The turbine efficiency was computed from the last stage efficiency which is based upon a low mass flow rate. This is conservative because the average mass flow in the turbine is about 20 percent higher than at the last stage exit.

MINIMIZING CONFIGURATIONS OVER POWER RANGE

From a commercialization viewpoint, a study was conducted to determine the number of basic radial outflow turbine designs that would be required to cover the power range between 100 KW and 5MW. The number of designs required depends upon the performance variation specified for each individual design.

In a fixed geometry turbine with a fixed set of Rankine cycle parameters, shaft speed should be held constant while varying power output to maintain good performance. This is because in a multistage design, the individual stages should remain matched by holding the inlet/exit velocity triangles constant.

For a sample case chosen, the analysis was begun with a 5 MW turbine design. Holding the shaft speed constant, the turbine blade heights (and thus power output) were reduced until the turbine efficiency had decreased by 3 percentage points. Turbine efficiency was computed by the methods described earlier. At the power level corresponding to the reduced power output of the fixed turbine design, the process was restarted with a new design. Shaft speed and turbine efficiency were recomputed for an optimized design.

A sample cycle with turbine inlet conditions of 1000°F and 1000 psia and a condensing temperature of 110°F was utilized for the analysis. The turbine family which resulted for the 5 MW to 100 KW power range is shown in Figure 29. With a 3 percentage point deviation between designs, seven ROF turbines are needed to cover the above power range. For lesser variations between designs, a nearly linear relationship exists, i.e., 20 designs would be required with only a 1 percentage point deviation on each design.

POWER CONVERSION SUBSYSTEM EFFICIENCY

The complete Power Conversion Subsystem (PCS) was analyzed to determine the amount of heat energy required to produce a given amount of electricity.

GEARBOX AND GENERATOR

Data was obtained for commercial gearbox and generator efficiencies as a function of power output. This data is shown plotted in Figure 30. As can be seen in Figure 30, gearbox/generator efficiency decreases at an increasing rate below the 1000 KW power level.

The power consumed by the gearbox lube pump was specified by the manufacturers to be approximately 0.05 percent of the output power. For the PCS efficiency calculations, the power consumption of this pump was assigned to a category of other PCS low power consumers which is discussed later. Most gearboxes have dual pumps; in some cases, one shaft driven and one motor driven, to prevent the loss of oil pressure which can be very damaging to this equipment.

BOILER FEED PUMP

Boiler feed pump power for the cycles of this study ranged between 0.2 to 1.5 percent of the turbine power output. The equation for feed pump power was defined as follows:

$$E_f = \frac{m\ (P_i - P_e)}{806000}$$

This equation is based upon a 70 percent pump efficiency. No electric motor efficiency was accounted for because this pump could potentially be shaft driven from either the turbine or gearbox. For the sample cycle used in this report having inlet conditions of 1000°F, 1000 psia and 110°F (1.275 psia) condensing, the feed pump power represents 0.8 percent of the power output.

CONDENSER

The steam condenser power consumption is dependent upon the type of unit selected, which is one of the following:

1. Direct contact, air-cooled
2. Cooling tower, evaporative-cooled
3. Shell and tube, water-cooled.

In the above list, equipment cost and power consumption increase from top to bottom. In the table below, the approximate cost of the three condenser types is shown as a function of the heat rejection load and the differential between condensing steam and ambient temperature.

CONDENSER TYPE	EQUIPMENT COST (DOLLARS-°F/BTU/HR)
Air-cooled	0.50
Evaporative	0.25
Water-cooled	0.05

The water-cooled condenser option is by far the most economical; however, very large quantities of water are required. The cooling water flow rate is defined as follows:

$$m_w = \frac{C}{500\ (\Delta T)}$$

For the sample engine shown in Figure 31, a cooling water flow of 317 GPM would be required for a water temperature of 70°F. Assuming a 100 ft. head for transport of the cooling water to the condenser and 50 percent pump/motor efficiency, the power required for the circulation pump would be:

$$E = \frac{m_w}{26.5}$$

For an air-cooled condenser, the power required to drive the cooling fan as a function of the heat rejection load and the differential between condensing steam and ambient temperature is as follows:

$$E = \frac{C}{6900\ (\Delta T)}$$

For the sample engine shown in Figure 31, the fan power consumption would be 36.8 KW for an 85°F ambient. This results in a loss factor of 0.963 on the steam Rankine cycle efficiency. For a water-cooled condenser, this factor would only be 0.988. The penalty factor for an evaporative cooling system would fall somewhere between the two above values. Prior to the start of the study, however, a decision was made not to evaluate cooling tower performance.

AUXILIARIES

Other PCS power consumers have been grouped into a category labeled "PCS Auxiliary Power." The estimated power consumption as a function of the overall power output of items in this category would be the following:

	PCS AUXILIARY	POWER REQUIRED/ POWER OUTPUT
1.	TGG* instrumentation and controls	0.0005
2.	TGG* lube pumps	0.0010
3.	Gearbox oil cooler water pump	0.0005
4.	Condenser vacuum pump	0.0025
5.	Steam generator instrumentation and controls	0.0005
6.	Total	0.0050

*Turbine/gearbox/generator.

As shown in the sample engine efficiency calculation which follows, a loss factor of 0.995 was applied to the cycle efficiency to account for the PCS auxiliary power consumption.

POWER CONVERSION SYSTEM EFFICIENCY

Shown in Figure 31 is a sample steam Rankine engine efficiency calculation sheet, which is based upon the steam Rankine cycle of Figure 10. Loss factors were computed as described above for the following:

1. Gearbox
2. Generator
3. Steam generator feed pump
4. Condenser
5. Plant auxiliaries.

For the sample calculation shown in Figure 31, the overall engine efficiency of the power conversion subsystem was calculated to be 0.309 for an air-cooled unit and 0.317 for a water-cooled unit. For a 1000 KW engine condensing at 110°F, which is compatible with air or water cooling, engine efficiency is shown as a function of turbine inlet conditions in Figures 32 and 33.

PART LOAD OPERATION AND PERFORMANCE

The ideal load curve, from an economic standpoint, for a solar electric powerplant would be to operate at or near full power all of the time. In the early systems, it may be possible to connect them to the electrical grid in such a manner that would permit this type of operation. Eventually, however, the system will have to be designed to respond to a load curve like that of the large electric utilities. Typically, this means an annual load factor of approximately 65 percent and the ability to turndown to 20 percent load. The capability to operate efficiently at part load is therefore an important design criteria.

Three methods of operating the steam Rankine engine at part load were investigated. These being the following:

1. Turbine inlet temperature held constant, inlet pressure throttled to match load.
2. Turbine inlet temperature and pressure decreased to match load.
3. Turbine inlet pressure held constant, inlet temperature decreased to match load.

For each of the above operating methods, a set of assumptions was applied; these include:

1. Turbine inlet volumetric flow rate held constant throughout the load range.
2. Condenser heat rejection load divided by the differential between condensing and ambient temperatures was held constant.
3. Turbine shaft speed was held constant. ETI and NA [illegible] urbine part load efficiency was used to define the ROF turbine off-design performance.
4. Gearbox losses were held constant; thus, gearbox efficiency decreases with load as shown in Figure 34.
5. Generator part load performance was taken from commercial data as shown in Figure 34.
6. Feed pump and condenser power requirements were computed as defined in the section on Power Conversion Subsystem Performance.
7. Control and instrumentation power were held at a constant value of 0.5 percent of the full load power output.

By holding the turbine inlet volumetric flow rate constant, the change in the turbine blade-jet (u/c) ratios is minimized during part load operation. This optimizes the turbine's off-design performance, as turbine efficiency is very sensitive to changes in this dimensionless parameter.

Operating the condenser as described in Point 2 above will cause the condensing temperature of the steam to decrease with load. Thus, as the load decreases, the specific volume of the turbine exhaust steam will increase maintaining a volumetric flow rate near the design value. This also will contribute to good turbine part load efficiency.

Turbine part load efficiency as a function of the number of stages and load is shown in Figure 35. A very key assumption is built into Figure 35, which is: all turbine stages are subsonic. Thus, the maximum design pressure ratio varies as a function of the number of stages. Using the equation defined previously, a chart showing pressure ratio vs. number of stages in Figure 35 can be derived.

Steam Rankine engine performance as a function of load was analyzed using the sample Rankine cycle of Figure 14 as a basis. The results of the analysis are shown plotted in Figure 36. The variable superheat (#3) method is not plotted because at part load, the moisture in the turbine exhaust steam was excessive from the standpoint of long turbine blade life. For most of the Rankine cycles of this study, this is likely to be the case for the variable superheat method, which can only be applied when the full load turbine exhaust is superheated steam.

The constant inlet temperature (#1) method produces the highest part load efficiency. In addition, this method has these advantages: (1) of the three methods, will draw down the storage subsystem to the lowest temperature, (2) requires a very simple control system, and (3) produces the least exposure of turbine to wet steam

Steam Rankine engine part load performance vs. the power output of the unit is shown in Figure 37. The results indicate that unit size is not a significant effect on the rate of deterioration of engine performance at part load. Also shown in Figure 37 is part load steam Rankine cycle performance, which is based only on turbine off-design efficiency from a throttled steam supply.

CONTROLS

ENGINE CONTROLS

This section will discuss the controls required for successful operation of the power conversion subsystem. Primary emphasis will be on the turbine/gearbox/generator.

Conventional hydraulic-mechanical governors operate at speeds below the 1800 rpm generator speed standard for the 100 KW to 5 MW power range. Thus, they require a small auxiliary gearbox mounted on the turbine or gearbox. Governor shaft power requirements are low, approximately 0.00025 of the turbine shaft power. Commercial equipment has the capability to respond to 0.02 percent change in speed. Other control capabilities include the following:

1. Synchronization of speed of multiple units.

2. Overspeed emergency shutdown actuation (Electrical Engineer's Handbook calls for a design limit of 110 percent maximum overspeed).

3. Operating range down to 25 percent of design speed.

When feedwater heating is used to improve engine efficiency, control of the turbine extraction ports must be considered. To maintain optimum turbine efficiency throughout the load range, it is necessary to control the extraction flows from the turbine.

For the case where single or dual extractions are used, commercially available electronic controls exist which will:

1. Modulate the turbine inlet and extraction valves to hold shaft speed constant.

2. Maintain turbine horsepower output at a fixed optimum value.

In large electric powerplants, which may have eight or more feedwater heaters, the turbine manufacturer will specify the extraction flows as a function of turbine power output. The correct extraction flows are then maintained by an operator.

In the design of a solar electric powerplant, several cost and reliability tradeoffs will have to be studied to determine the best approach. Earlier, a statement was made that the addition of feedwater heaters will always be economic on a system's basis. However, this may not be true if fully automatic control is required. The cost of addition of the Nth feedwater heater control logic may become prohibitive. The reliability of this complex automatic control would have to be traded off against that of the solar receiver it would replace. In the case where the system has storage, excess energy at part load is likely to be available. In that case, uncontrolled extraction ports could be utilized.

According to the Edison Electric Institute, the three major causes of turbine failure are the following:

1. Solid particle erosion (from steam generator tube exfoliation).

2. Water induction (through feedwater extraction lines).

3. Corrosion (from water impurities).

The problem of water induction can largely be overcome by placing check valves in the feedwater extraction lines, and by isolating the turbine from the steam generator during startup and shutdown. The other two problems are related principally to material selection and water quality control.

Both Babcock and Wilcox and Combustion Engineering recommend the use of a demineralizer system for use with the once-through type steam generators likely to be used for solar electric power generation. A deep bed of hydrogen or ammonium cations is used to remove ionized solids from the system. This method of water quality control is also known as condensate polishing.

SYSTEM CONTROL AND POWER OUTPUT

To achieve the most cost effective solar electric power system, a configuration and operating method must be devised which derives the optimum power output from a fixed collector field. A key design feature of any system is the optimum value for this ratio:

$$R = \frac{\text{Powerplant Nameplate Rating}}{\text{Solar Receiver Design Output}}$$

First order effects on the above ratio come from the following:

1. Average system load
2. Length of the operating period
3. Collector output vs. time of day
4. Power conversion system efficiency vs. output.

It is beyond the scope of this study to provide detailed analysis of the above design problem, which will dictate the control strategy to be used. However, some basic systems were investigated to illustrate the interaction of the above factors.

To analyze the R ratio above, the energy requirements of the total solar electric powerplant must be known. A study contained in Reference 4 estimated the plant auxiliary power, exclusive of that required by the PCS, to be approximately 4 percent of the plant nameplate rating. The plant auxiliary power should remain relatively constant and independent of PCS output. PCS and plant performance vs. load are shown in Figure 38. Note that in Figure 38 the full load efficiency of the PCS and the plant has been set equal to 100 percent. Thus, the curves shown represent the rate of degradation of performance.

On a given day for a system having only buffer type storage, the optimum solar receiver/PCS combination occurs at an R value on one. This is due to the shape of the solar insolation vs. time of day curve. A sample curve representing insolation at Barstow, California, the site of DOE's 10 MWe pilot solar electric plant, is shown in Figure 39. From sunrise to sunset, the relative receiver effectiveness as a function of R value is as follows:

POWERPLANT RATING	R VALUE	ELECTRICAL OUTPUT	ELECTRICAL OUTPUT ÷ RECEIVER SIZE
1.00	1.00	1.00	1.00
1.00	0.80	1.08	0.86
1.00	0.40	1.22	0.49

For this minimal storage type system, decreasing the R value increases the daily output of a given PCS unit. However, this increase is relatively insignificant compared to increase in size of the solar receiver. This would be economically undesirable.

CONCLUSIONS

This report covers the results of a study investigating the application of ETI's radial outflow (ROF) turbine to solar steam Rankine engines.

Over the range of engine parameters studied, it was found that high efficiency multi-stage ROF turbine designs could be achieved with the speed capability of commercial gearboxes and electric generators. An overhung turbine/gearbox configuration would be possible in most cases, all turbine stages being located on a single disc.

For the steam Rankine cycles of interest, the moisture tolerance of the expander is an important design criteria. Much data is available regarding this design limitation with axial flow turbomachinery. However, it is suspected that this data may be somewhat conservative when applied to the ROF turbine geometry. When high turbine inlet pressure is utilized, reheating of the steam will be required in many cases to maintain control of the moisture in the expander.

In solar steam Rankine engines, the use of steam extracted from the turbine for feedwater heating can produce the following results:

1. Improvement of cycle efficiency up to 10 percent, yielding savings in solar receiver size and total system cost.
2. Reduction in condenser size, effecting savings in system cost especially in cases where air-cooled condensing is utilized.
3. Reduction in turbine blade height on last stage, lowering principal stress factor in turbine.

For the above reasons, feedwater heating should be included in any solar steam turbine driven Rankine engines.

The method of operation and control of the solar steam engine can have significant effects on the gross power output over an operating period. Points to consider are the following:

1. Engine performance is more sensitive to turbine inlet temperature variations than inlet pressure variations.
2. Engine efficiency decreases at an increased rate below 20 percent of full load.
3. Engine off-design operating procedure should not cause moisture in the expander to exceed the design limiting value.

In the 100 KW to 5 MW power range, a steam Rankine engine with a ROF turbine primemover should deliver 30 percent conversion efficiency of heat input to electrical power output including losses when turbine inlet temperature exceeds 1000°F and condensing temperature is 110°F or less. The only major developmental item needed to produce such a system being the ROF turbine. The technology base developed from work on smaller ROF turbines, however, considerably reduces the time and risk elements associated with the development of the turbines discussed in this study.

SYMBOLS

A	flow area; ft^2
b	exit blade height; ft
C	steam engine heat rejection load; Btu/hr
D_h	hydraulic diameter; ft
E	power output; KW
E_f	boiler feed pump power; KW
g	gravitational constant; 32.2 ft/sec^2
$\Delta h'$	actual stage total enthalpy change; Btu/lb
Δh_i	ideal turbine expansion enthalpy change; Btu/lb
Δh_t	turbine inlet enthalpy minus actual exit enthalpy; Btu/lb
Δh_w	turbine inlet enthalpy in wet region; Btu/lb
J	conversion constant; 778 ft-lb/Btu
K	kinematic viscosity; ft^2/sec
M	stage mach number
m	mass flow rate; lb/hr
m_e	extraction mass flow rate; lb/hr
m_i	inlet mass flow rate; lb/hr
m_w	water flow rate; gpm
N	shaft speed; rpm
P_e	exit pressure; psia
P_i	inlet pressure; psia
P_x	extraction pressure; psia
Q	steam quality
Re	Reynolds number
r_t	turbine tip radius; ft
S	blade stress; psi
T	temperature; °F

T_x	saturation temperature at Px; °F
V	velocity; ft/sec
V_{sp}	spouting velocity; ft/sec
V_t	tip velocity; ft/sec
W	wetted perimeter; ft
X	number of turbine stages
Z	overall (dry) turbine efficiency/last stage efficiency
α	Gymarthy's Factor = 0.35
λ	stage speed-work parameter
$\bar{\lambda}$	overall speed-work parameter
η_d	dry turbine efficiency
η_l	last stage efficiency
η_w	wet turbine efficiency
μ	viscosity; lb/ft-sec
ν	specific volume at turbine exit; ft^3/lb
ρ	density; lb/ft^3

FIGURE 1

RADIAL OUTFLOW TURBINE

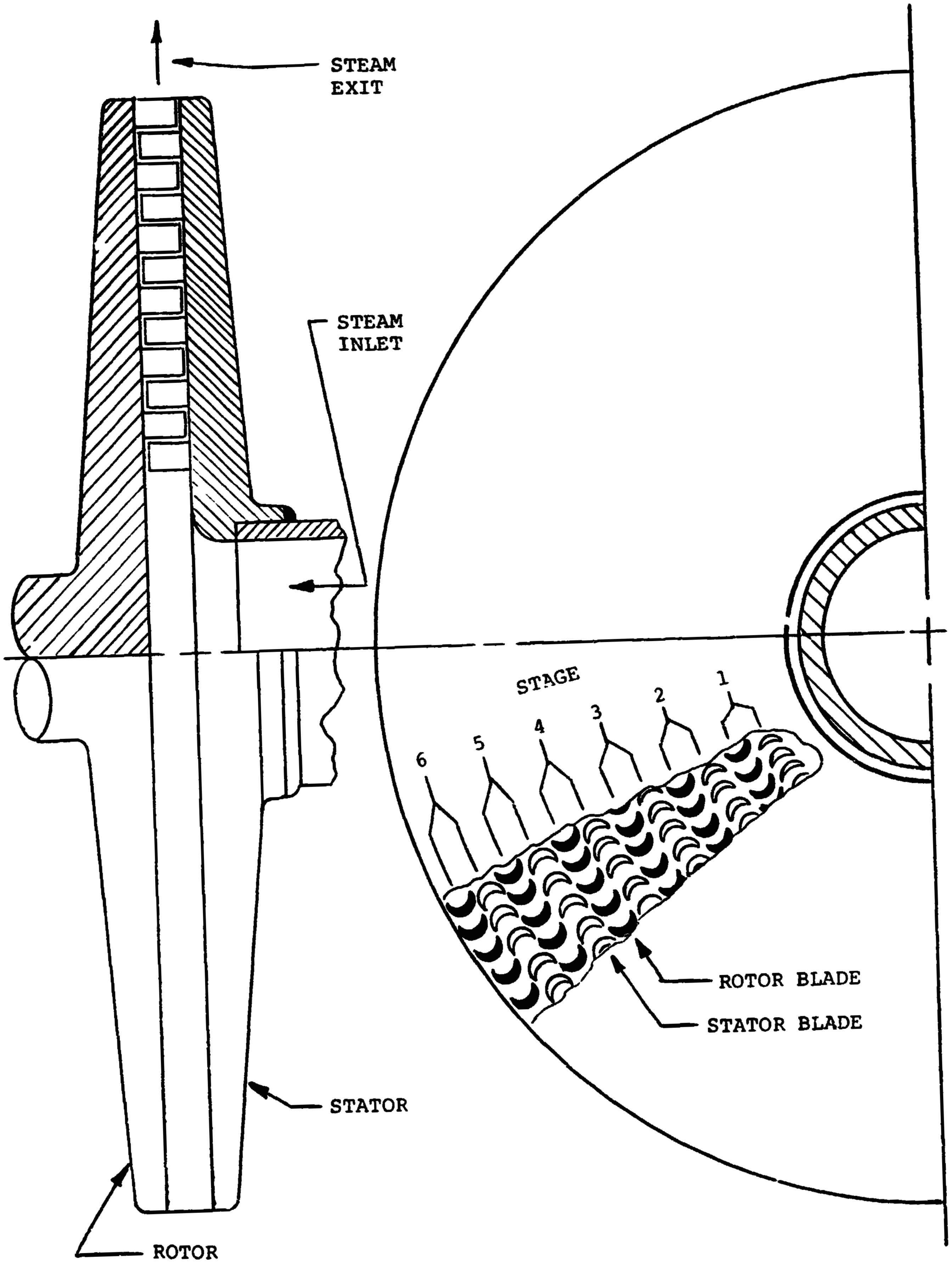
STEAM EXIT
STEAM INLET
STAGE
1
2
3
4
5
6
ROTOR BLADE
STATOR BLADE
STATOR
ROTOR

FIGURE 2

ETI TURBINE/GEARBOX LAYOUT

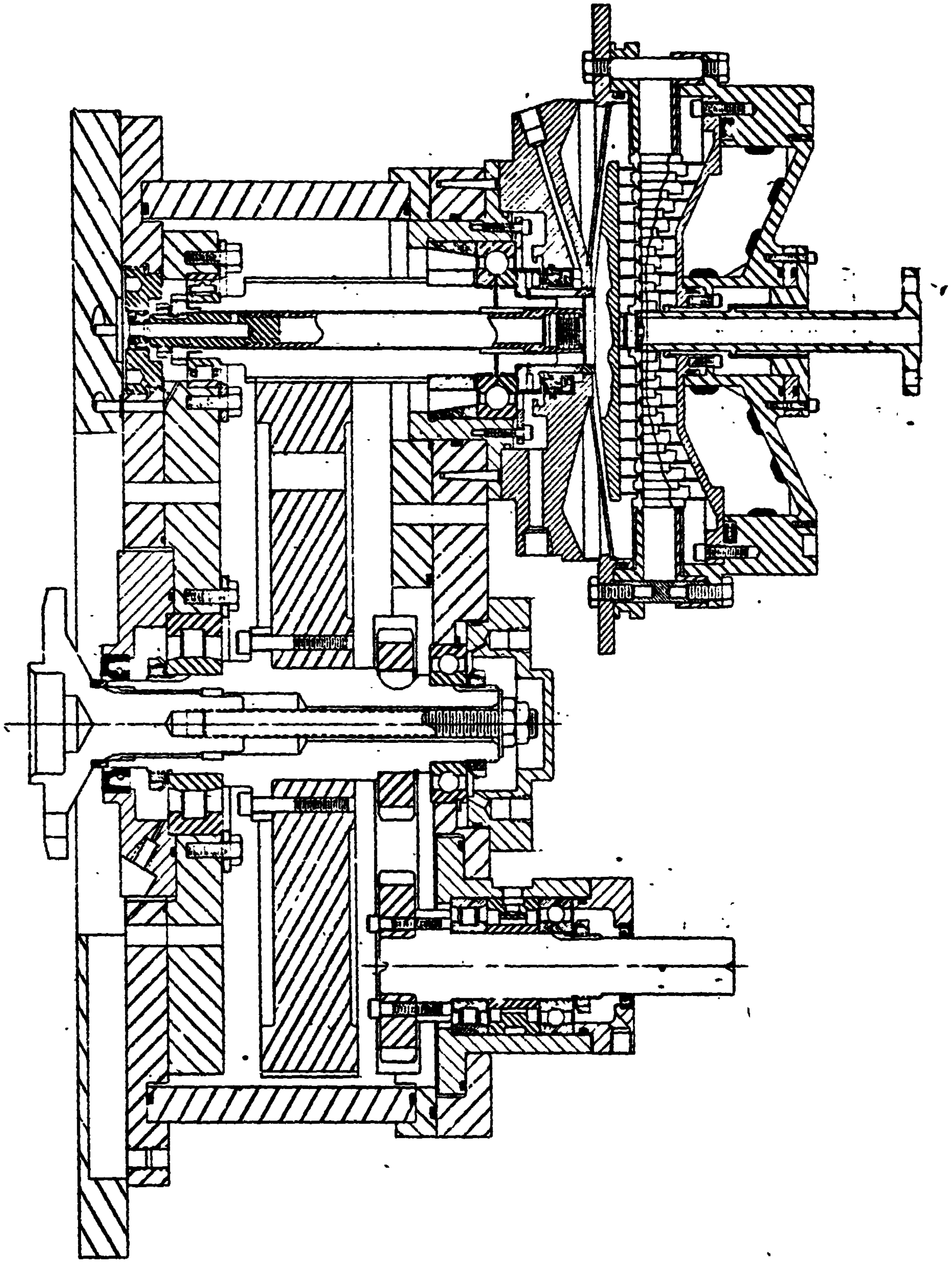

ORIGINAL PAGE IS
OF POOR QUALITY

FIGURE 3

TURBINE SINGLE STAGE PERFORMANCE REFERENCES

NO.	NTIS NO.	AUTHOR	TYPE
1	N71-17354	KOFSKEY	RADIAL
2	N70-10746	KOFSKEY	AXIAL
3	AD-859-702L	NICHOLS	AXIAL
4	N68-37263	FUTRAL	AXIAL
5	N68-18501	NUSBAUM	AXIAL
6	N68-16228	KLASSEN	AXIAL
7	N67-17626	NUSBAUM	RADIAL
8	N67-16694	HOLESKI	RADIAL
9	N67-15558	ODIVANOV	RADIAL
10	N67-10799	KOFSKEY	RADIAL
11	AD-642-767	BALJE	AXIAL
12	N66-16056	KOFSKEY	RADIAL
13	N66-15642	WASSERBAUER	RADIAL
14	N62-14819	WONG	AXIAL

FIGURE 4

TURBINE EFFICIENCY VS. REYNOLDS NUMBER

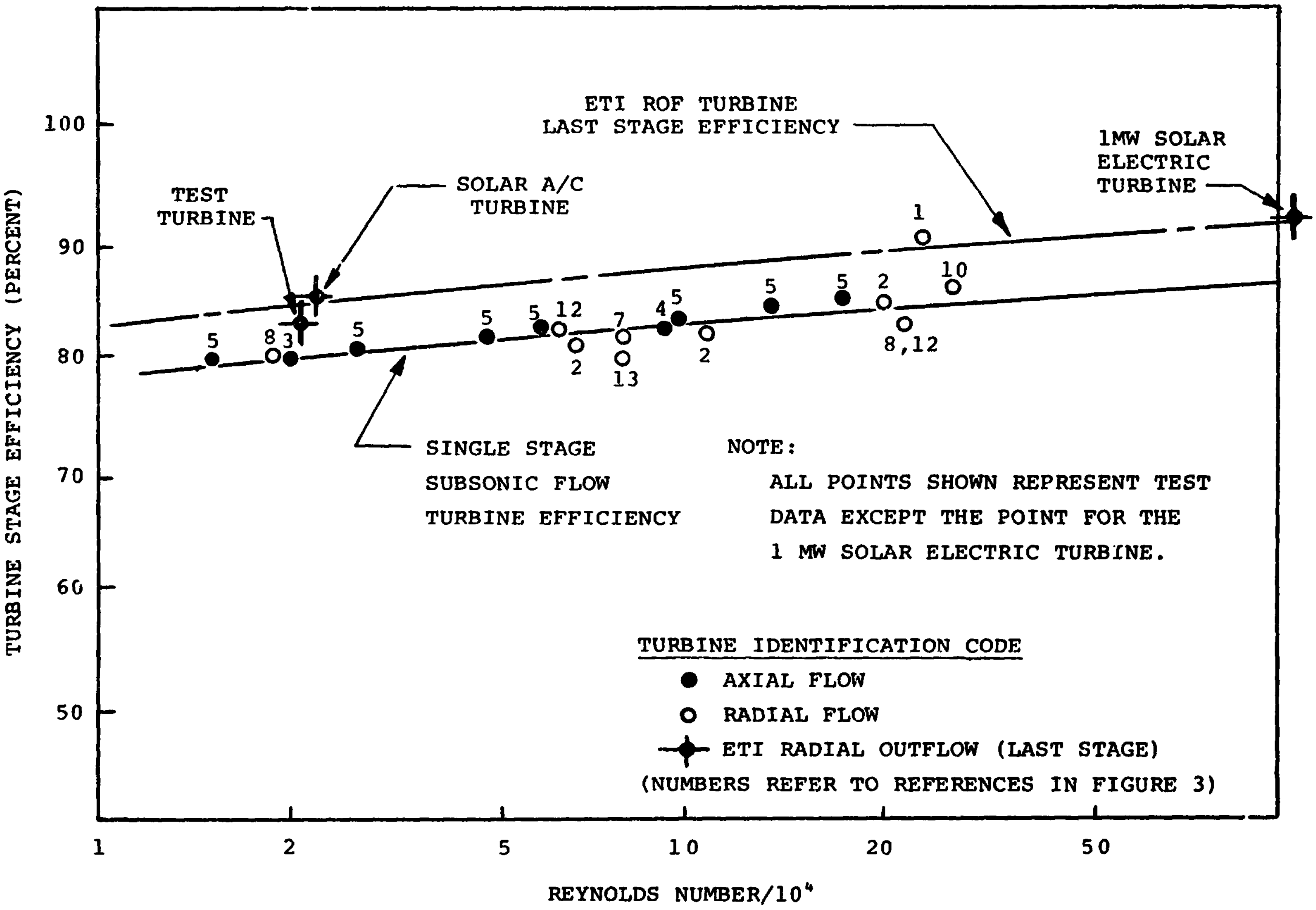

NOTE:

ALL POINTS SHOWN REPRESENT TEST DATA EXCEPT THE POINT FOR THE 1 MW SOLAR ELECTRIC TURBINE.

TURBINE IDENTIFICATION CODE

- ● AXIAL FLOW
- ○ RADIAL FLOW
- ✦ ETI RADIAL OUTFLOW (LAST STAGE)

(NUMBERS REFER TO REFERENCES IN FIGURE 3)

FIGURE 5

OVERALL TURBINE EFFICIENCY VS. LAST STAGE EFF. & NO. OF STAGES

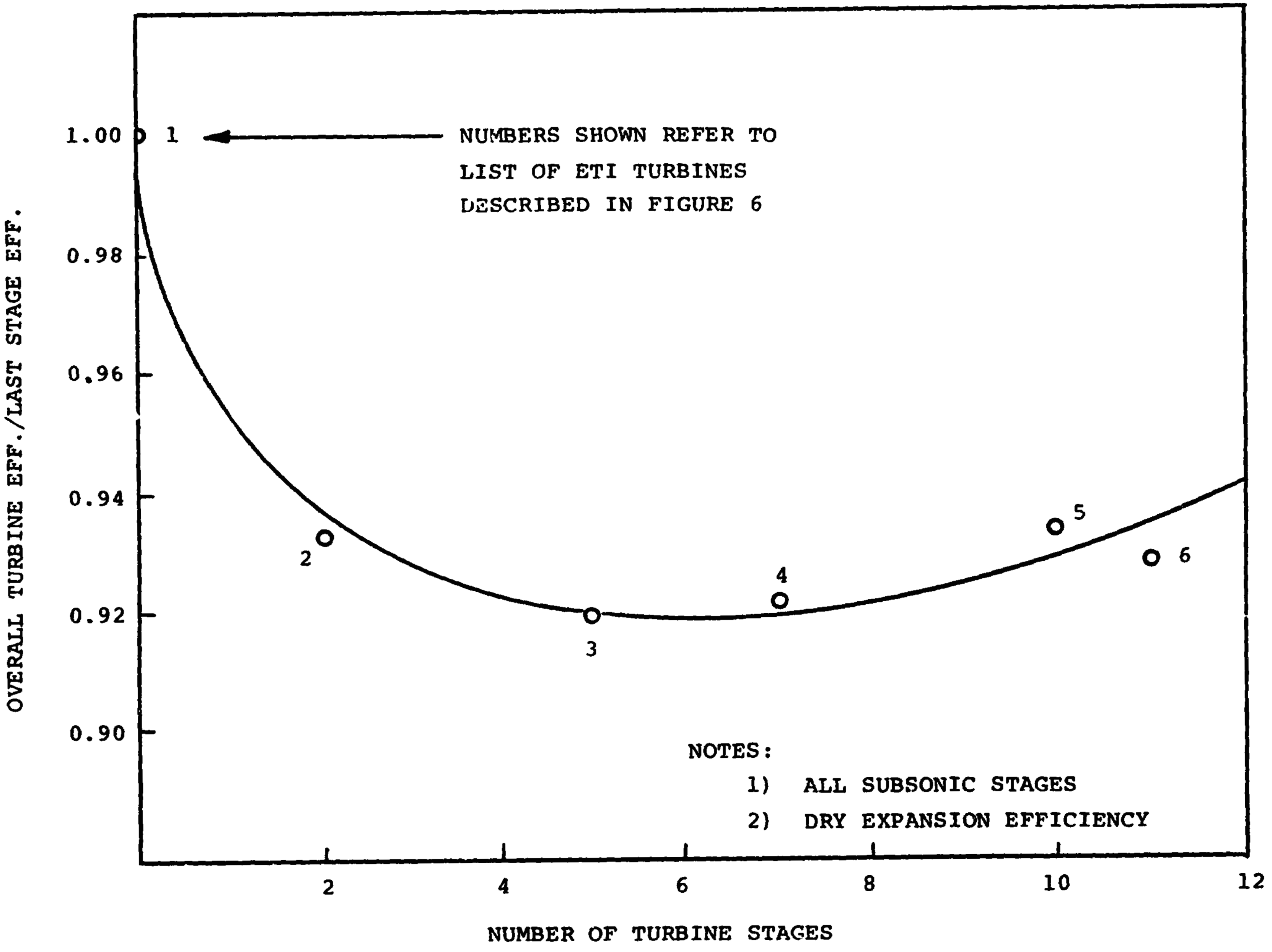

FIGURE 6

ETI RADIAL OUTFLOW TURBINE
LAST STAGE EFFICIENCY/TURBINE EFFICIENCY, (Z FACTOR)

REFERENCE NUMBER	NO. OF STAGES	ETI ROF TURBINE DESCRIPTION	LAST STAGE EFF.	TURBINE EFF.
1	1	All single stage turbines	-	-
2	2	8 KW test turbine of 1976	0.74	0.69
3	5	22 KW solar cooling turbine of 1979	0.85	0.78
4	7	9 KW gas heat pump turbine of 1975	0.65	0.60
5	10	68 KW automotive turbine of 1973	0.75	0.70
6	12	1100 KW solar electric turbine of 1979	0.94	0.90

FIGURE 7

IDEAL TURBINE EXPANSION

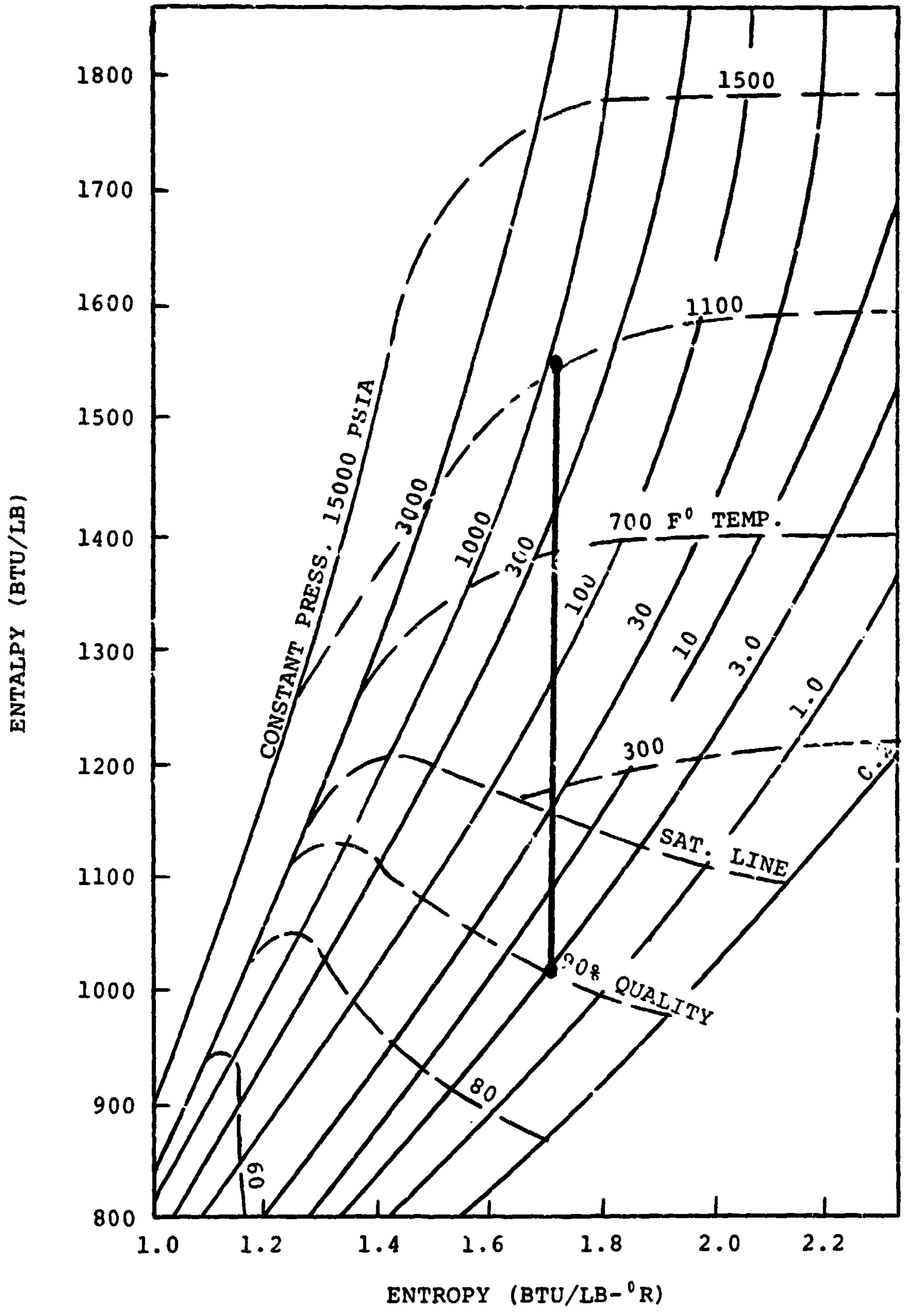

FIGURE 8

EXAMPLES OF TURBINE MOISTURE IN UTILITY POWERPLANT PRACTICE

PLANT NAME	OWNER	TURBINE EXHAUST QUALITY
Bruce Mansfield	Ohio Edison	0.918
Bayshore	Toledo Edison	0.911
Yankee	Rowe	0.848
(Struthers)	Duquesne Power	0.890
(Struthers)	Texas Utilities	0.915

FIGURE 9

GEARBOX SHAFT SPEED VS. POWER LEVEL

REF. NO.	POWER RATING (KW)	MANUFACTURER AND MODEL NUMBER	MAXIMUM PINION SPEED	NUMBER OF REDUCTIONS	OUTPUT SPEED
1	280	COTTA-412D	19,200	2	1800
2	375	COTTA-712D	17,400	2	1800
3	1000	WESTERN-11406	11,700	1	1800
4	5000	WESTERN-12212	10,400	1	1800
5	1390	LOHMAN-ITG32H	12,600	1	1800
6	373	SUNDYNE-SKO	11,700	1	1800
7	130	COTTA-215D	30,600	2	3600
8	750	WESTERN-11104	13,700	1	1800
9	810	LOHMAN-ITG25H	13,500	1	1800
10	1877	FALK-IIPC	9,000	1	1800

FIGURE 10

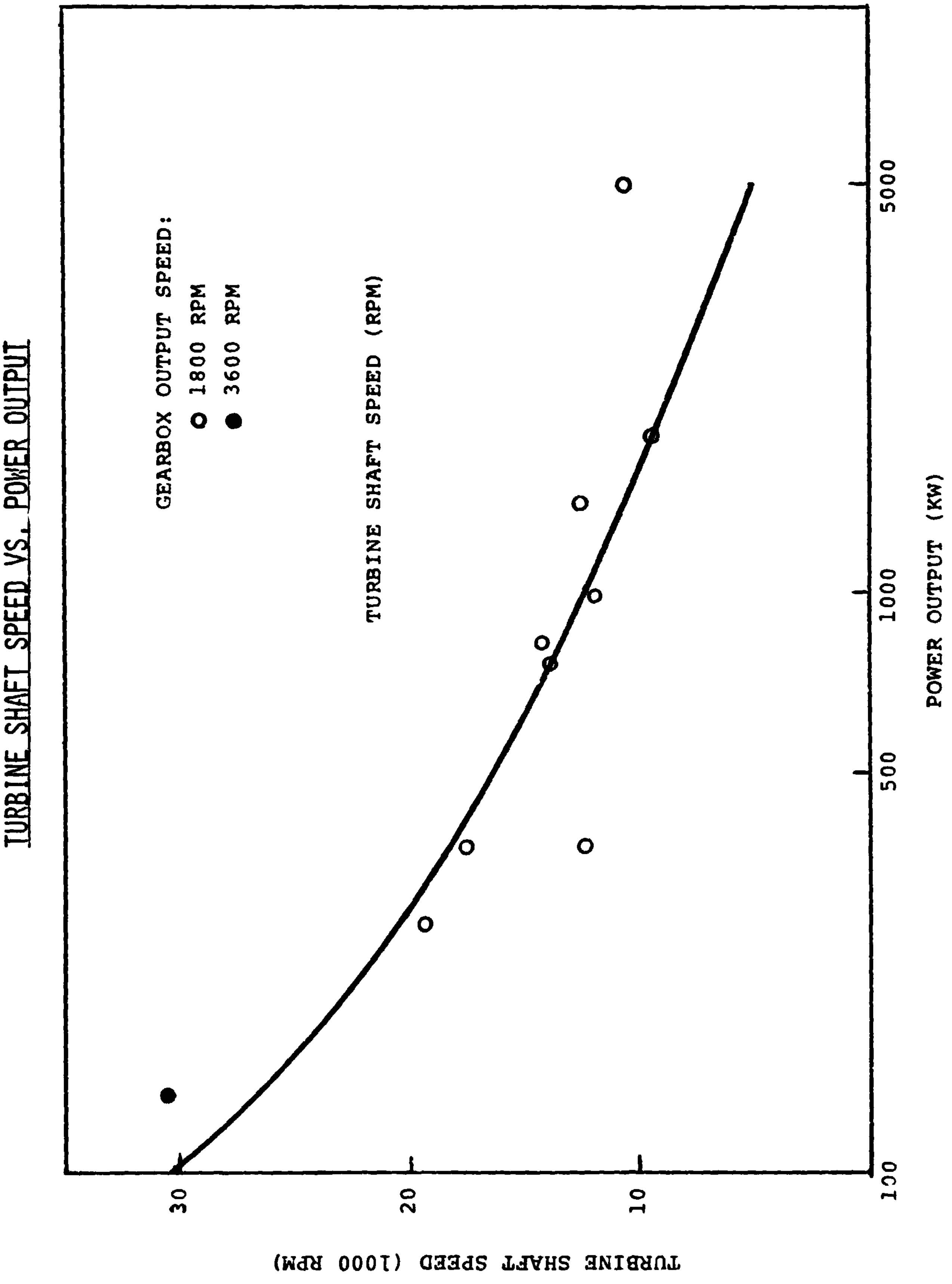

TURBINE SHAFT SPEED VS. POWER OUTPUT

FIGURE 11

TURBINE EFFICIENCY VS. NUMBER OF STAGES

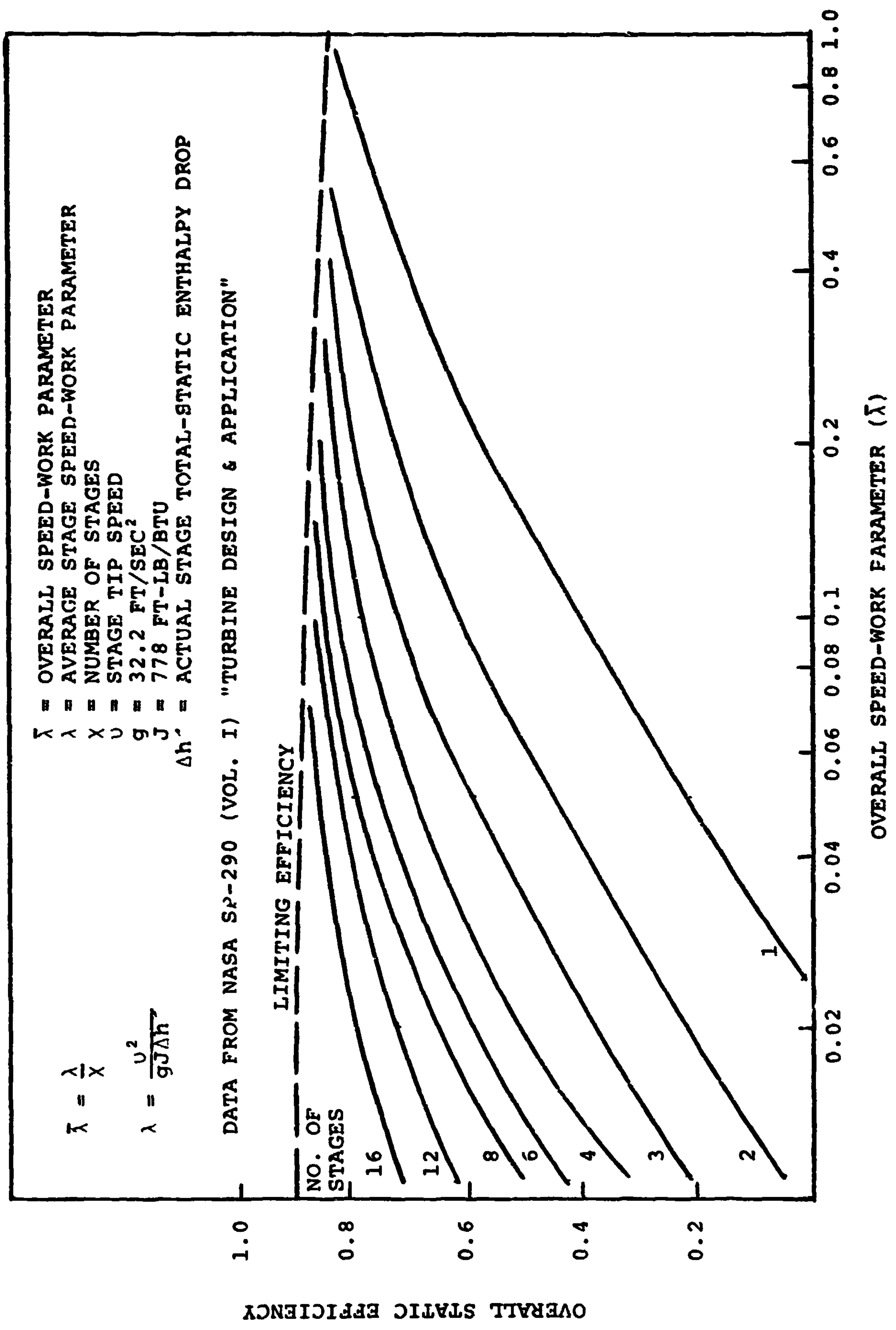

FIGURE 12

STEAM RANKINE ENGINE PERFORMANCE VS. NUMBER OF TURBINE STAGES

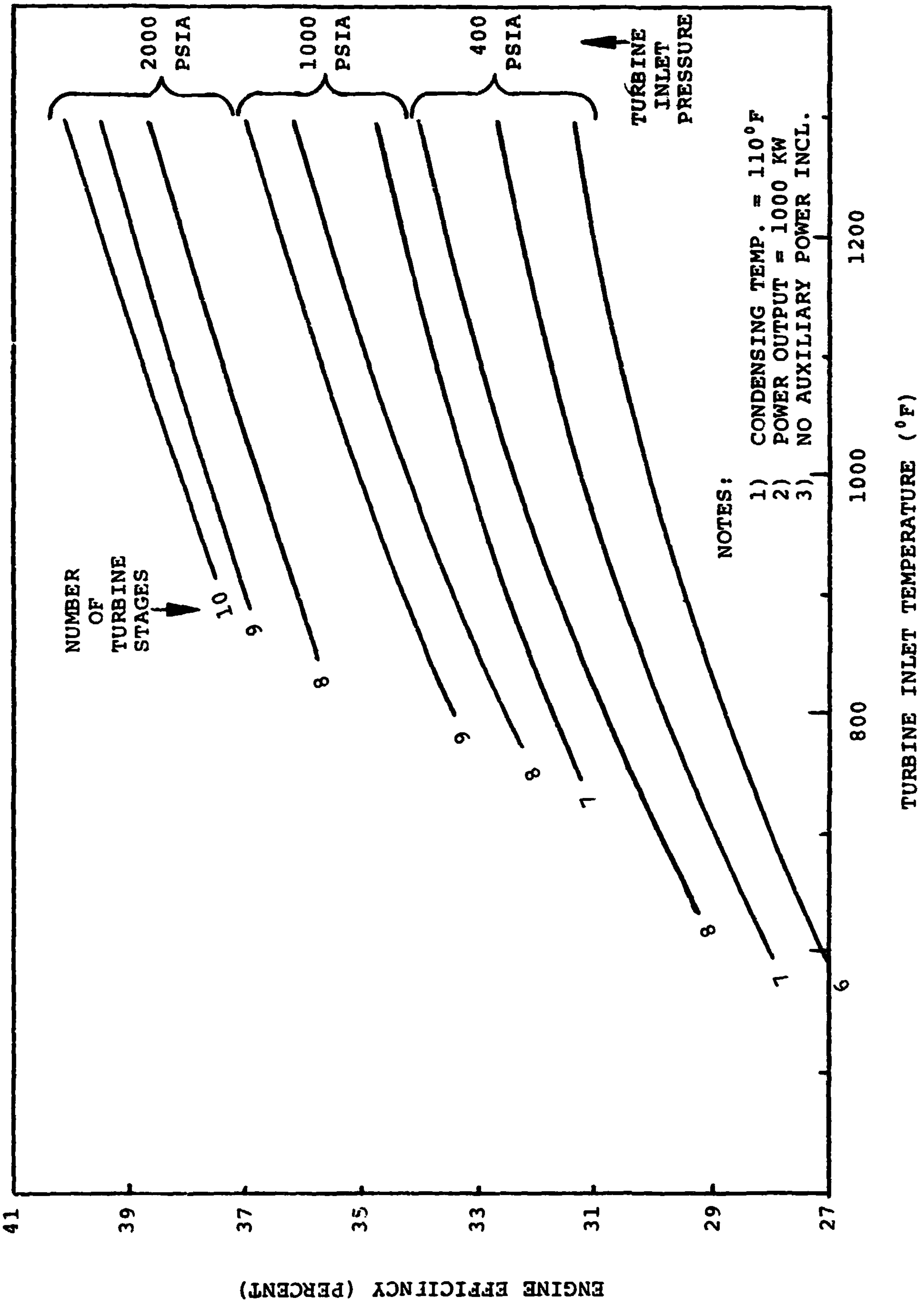

NOTES:
1) CONDENSING TEMP. = 110°F
2) POWER OUTPUT = 1000 KW
3) NO AUXILIARY POWER INCL.

FIGURE 13

BASIC STEAM RANKINE CYCLE

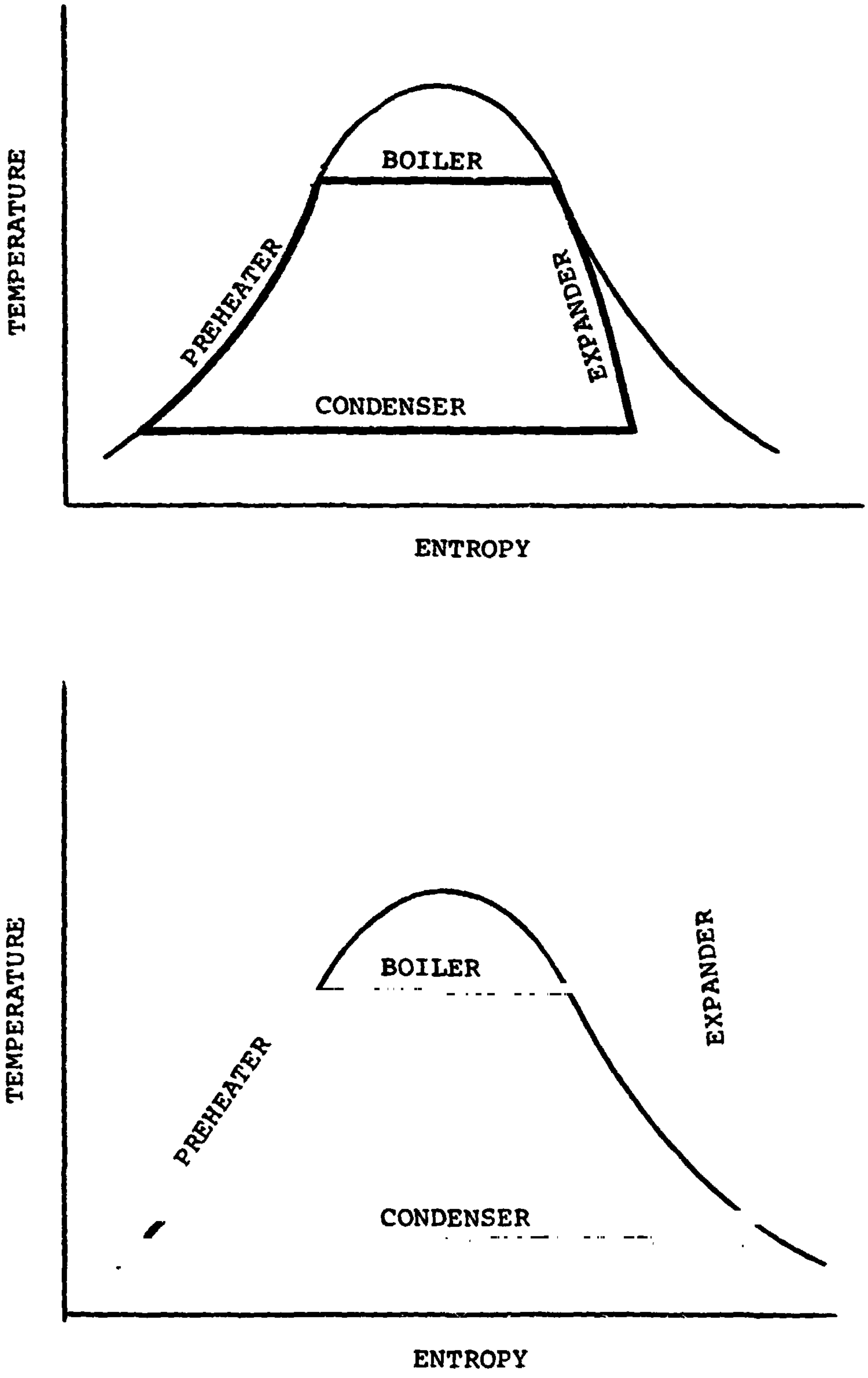
TEMPERATURE
BOILER
PREHEATER
EXPANDER
CONDENSER
ENTROPY
TEMPERATURE
BOILER
PREHEATER
EXPANDER
CONDENSER
ENTROPY

FIGURE 14

STEAM RANKINE CYCLE CALCULATION SHEET

TURBINE SPECIFICATIONS:

INLET: TEMPERATURE (°F) 1000 ENTHALPY (BTU/LB) 1505.4

PRESSURE (PSIA) 1000 ENTROPY (BTU/LB-°R) 1.6530

EXIT: PRESSURE (PSIA) 1.275 ENTHALPY (BTU/LB) 936.0

CONDENSING TEMPERATURE (°F) 110

POWER OUTPUT (HP) 1341 (KW) 1000

SHAFT SPEED (RPM) 12,000

ACTUAL EXIT: ENTHALPY (BTU/LB) 1010.6 QUALITY 0.904

SPECIFIC VOLUME (FT^3/LB) 240.1

MASS FLOW RATE (LB/HR) 6894

SPOUTING VELOCITY (FT/SEC) 1124.5

REYNOLDS NO. LAST STAGE 1.384×10^6

STAGE EFFICIENCY 0.947

EFFICIENCY (INCL. MOISTURE PENALTY) 0.869

RANKINE INGINE DATA:

HEAT INPUT (BTU/HR) 9.83×10^6

WORK OUTPUT (BTU/HR) 3.41×10^6

HEAT REJECTED (BTU/HR) 6.42×10^6

CYCLE EFFICIENCY 0.347

FIGURE 15

ACTUAL TURBINE EXPANSION

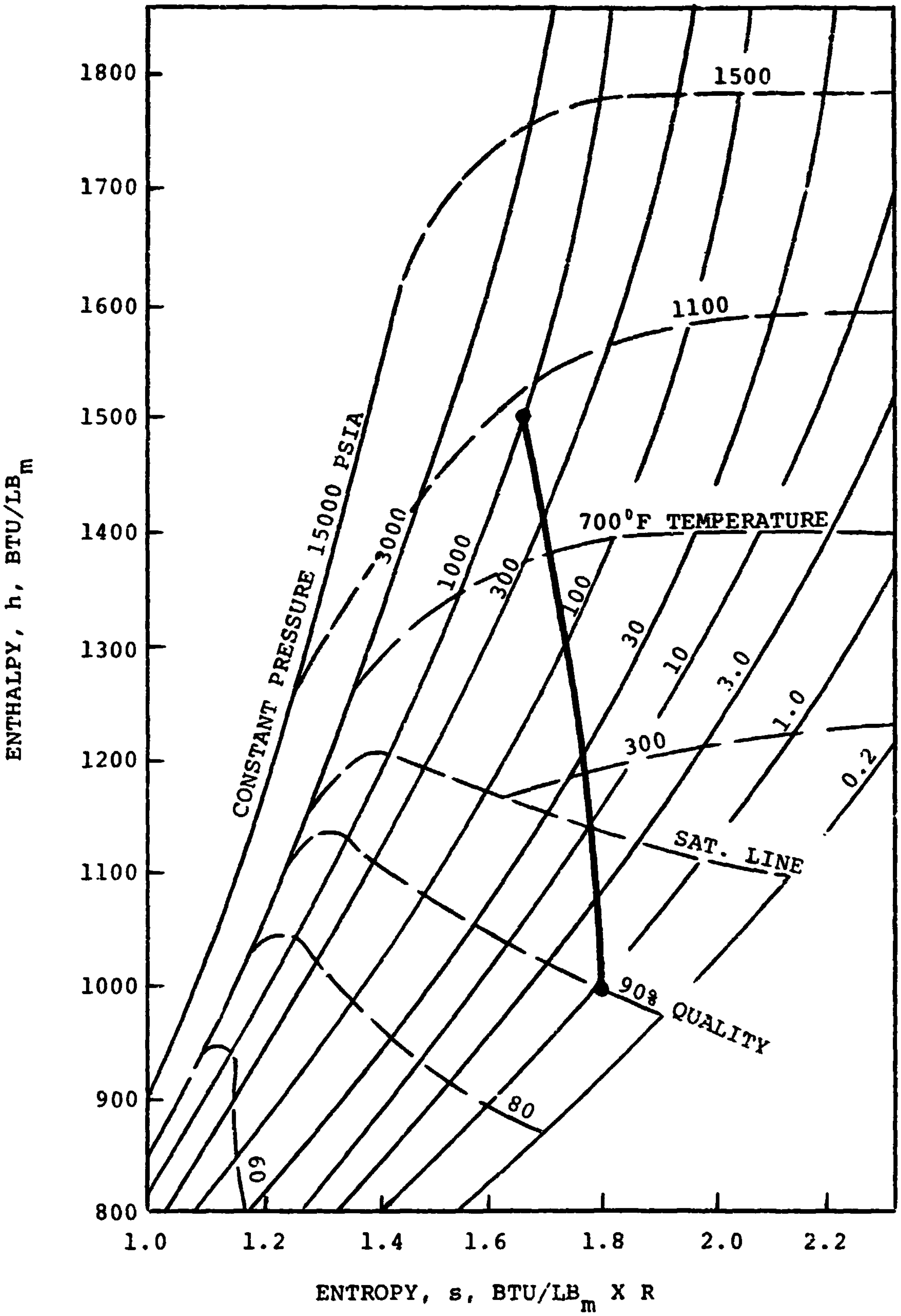

FIGURE 16

STEAM RANKINE (BASIC) ENGINE PERFORMANCE VS. TEMP/PRESS/POWER OUTPUT

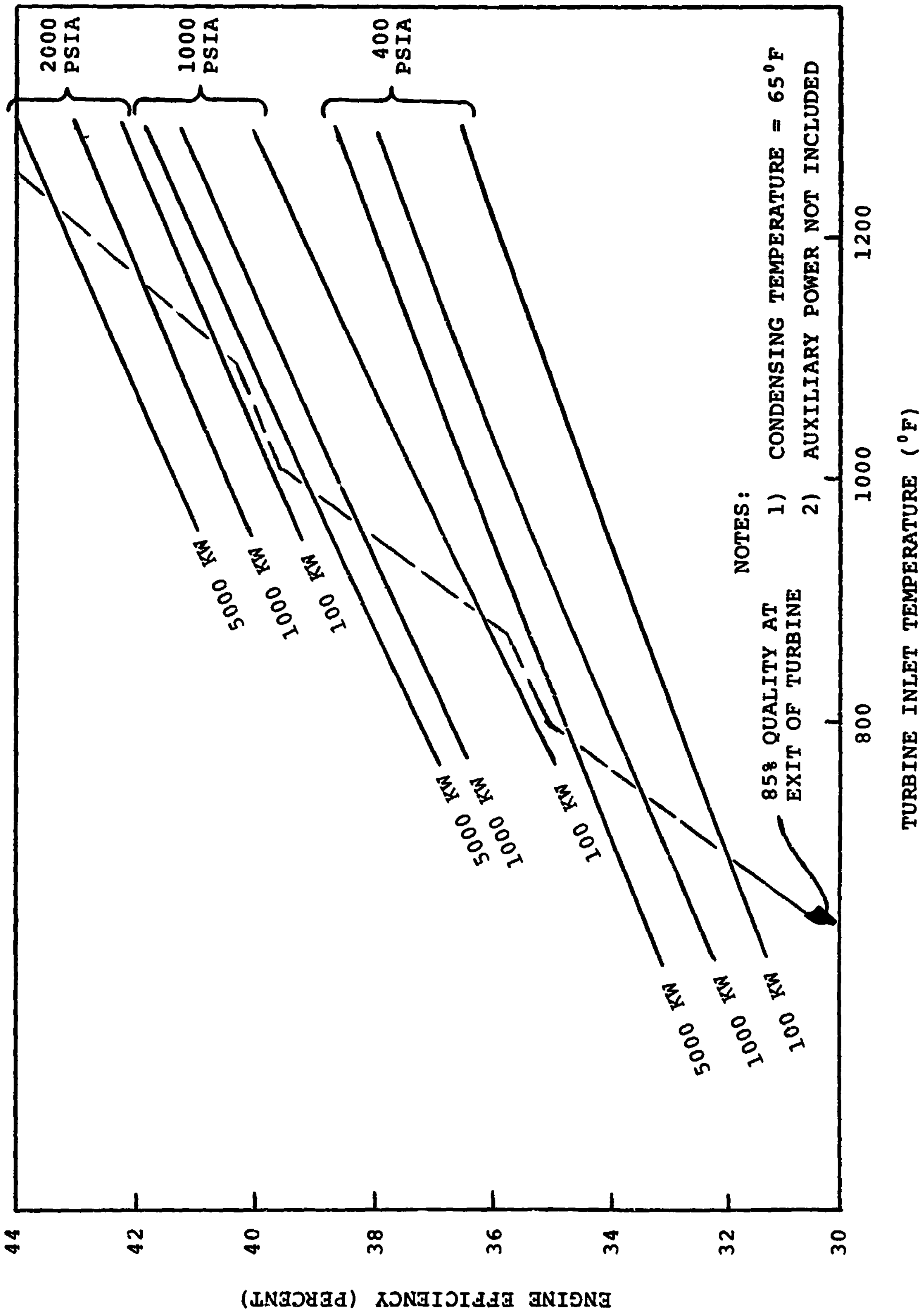

NOTES:

1) CONDENSING TEMPERATURE = 65°F
2) AUXILIARY POWER NOT INCLUDED

FIGURE 17

STEAM RANKINE (BASIC) ENGINE PERFORMANCE VS. TEMP/PRESS/POWER OUTPUT

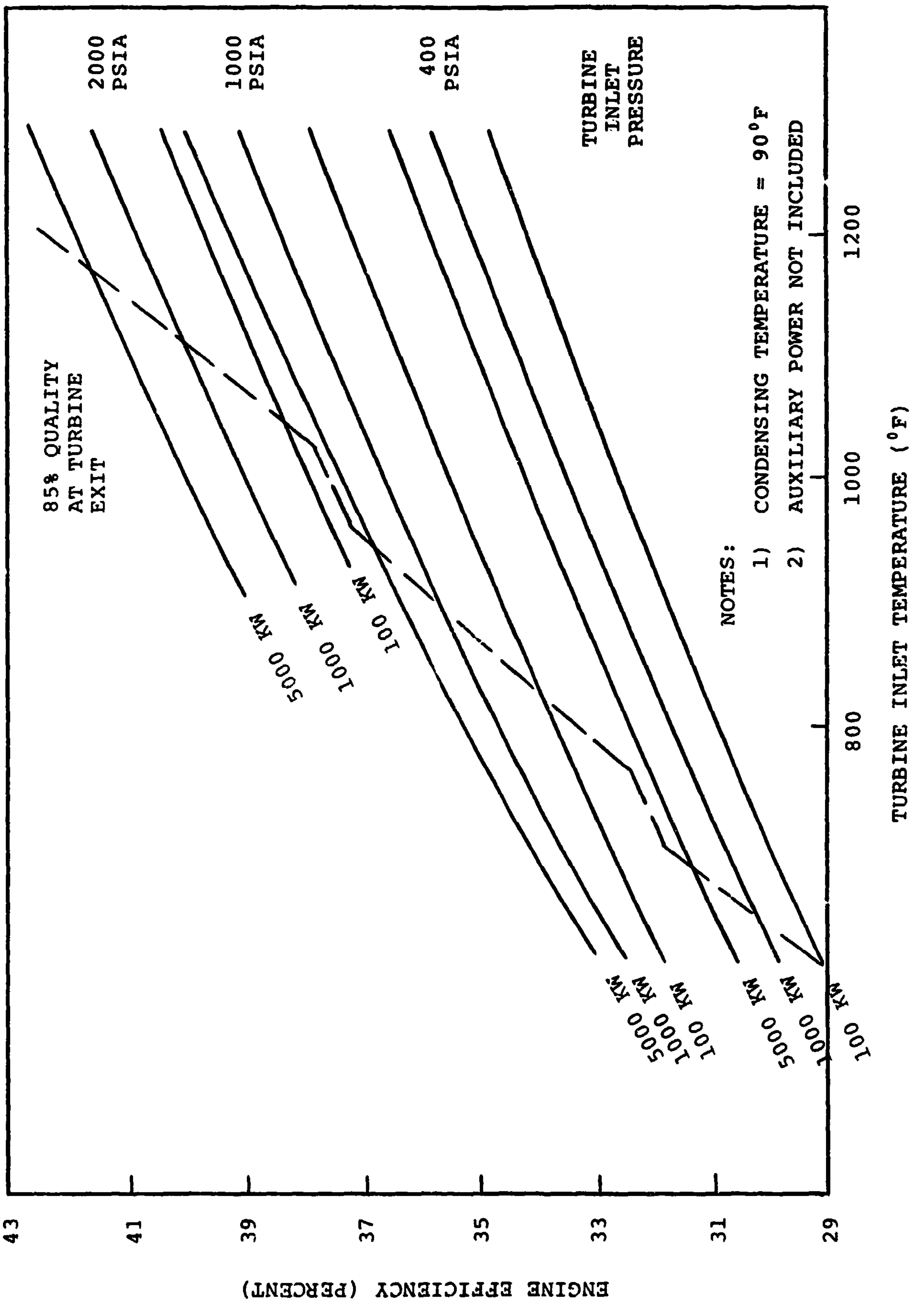

FIGURE 18

STEAM RANKINE (BASIC) ENGINE PERFORMANCE VS. TEMP/PRESS/POWER

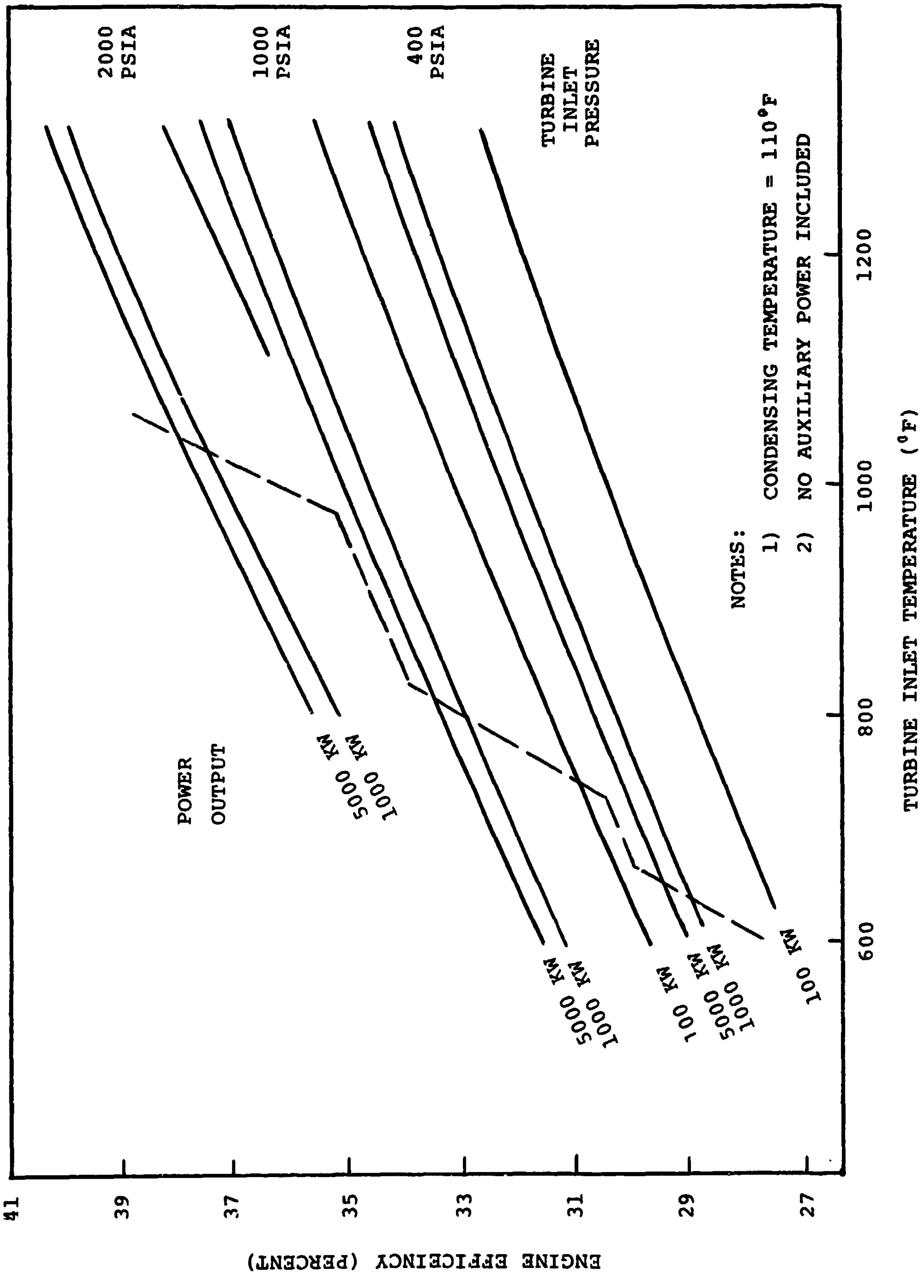

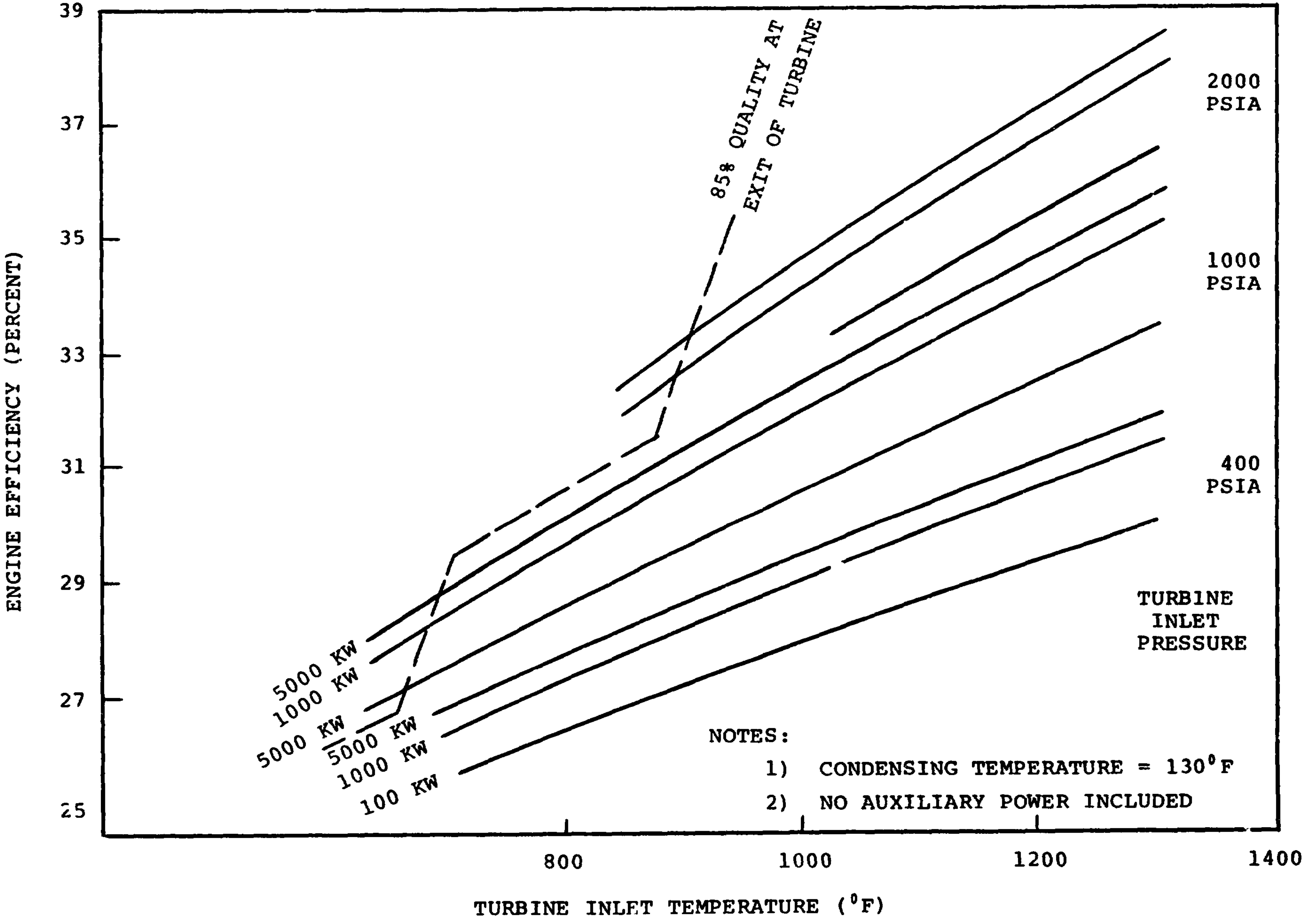

FIGURE 19

STEAM RANKINE (BASIC) ENGINE PERFORMANCE VS. TEMP/PRESS/POWER

FIGURE 20

STEAM RANKINE (BASIC) ENGINE PERFORMANCE VS. TEMP/PRESS/POWER

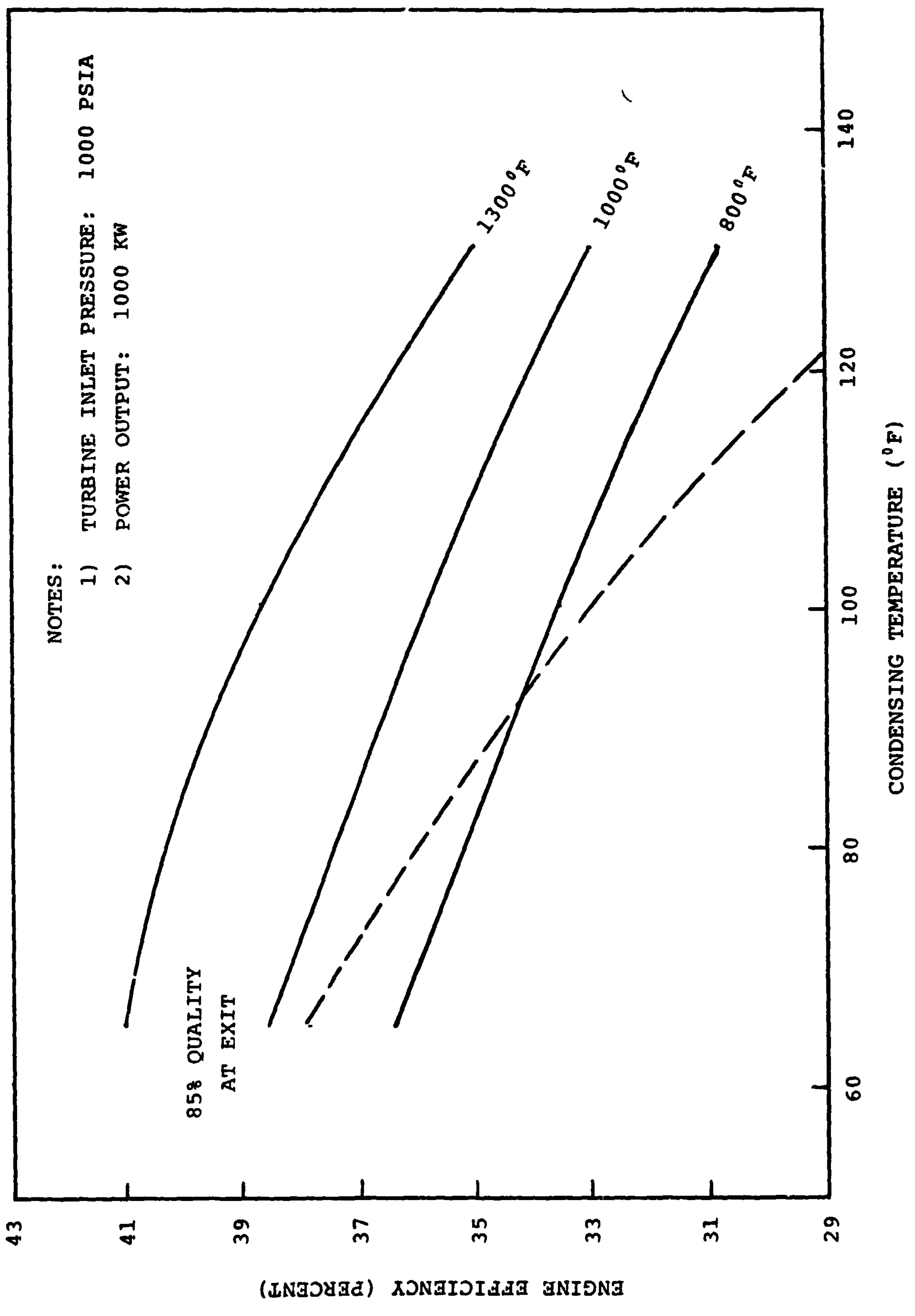

FIGURE 21

REHEATED STEAM RANKINE CYCLE

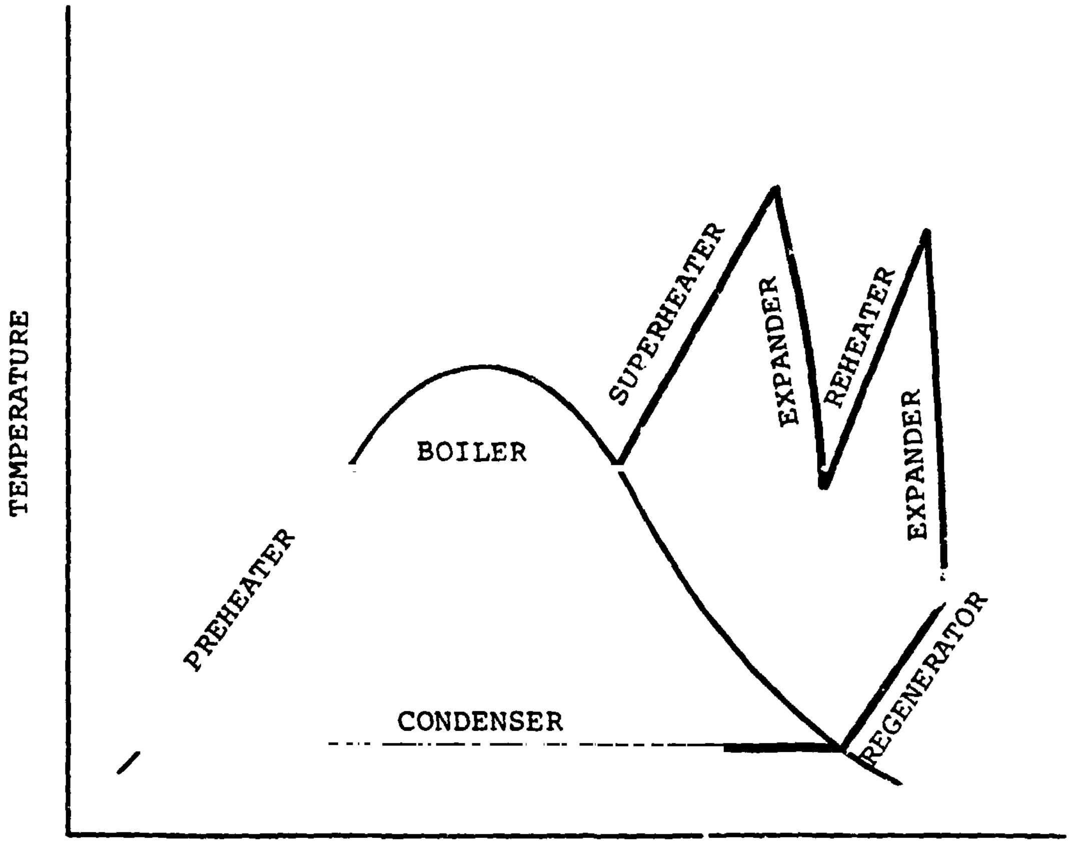
TEMPERATURE
ENTROPY
PREHEATER
BOILER
SUPERHEATER
EXPANDER
REHEATER
EXPANDER
REGENERATOR
CONDENSER

FIGURE 22

REHEATED STEAM RANKINE CYCLE CALCULATION SHEET

TURBINE SPECIFICATIONS:

INLET: TEMPERATURE (°F) 1000 ENTHALPY (BTU/LB) 1505.4

PRESSURE (PSIA) 1000 ENTROPY (BTU/LB-°R) 1.6530

EXIT: PRESSURE (PSIA) 36 ENTHALPY (BTU/LB) 1144.7

REHEAT: TEMPERATURE (°F) 950 ENTHALPY (BTU/LB) 1508.2

PRESSURE (PSIA) 35 ENTROPY (BTU/LB-°R) 2.0193

EXIT: PRESSURE (PSIA) 1.275 ENTHALPY (BTU/LB) 1146.9

{CONDENSING TEMPERATURE (°F) 110 }

POWER OUTPUT (HP) 1341 (KW) 1000

SHAFT SPEED (RPM) 12,000

ACTUAL EXIT:	1ST EXPANSION	2ND EXPANSION
ENTHALPY	1229.5	1200.0
QUALITY	1+	1+
SPECIFIC VOLUME (FT^3/LB)	13.8	359.0
MASS FLOW RATE (LB/HR)	5840.0	5840.0
SPOUTING VELOCITY (FT/SEC)	1550.0	1500.0
REYNOLDS NO. LAST STAGE	8150.0	5.510×10^5
STAGE EFFICIENCY	0.826	0.924
EFFICIENCY (INCL. MOISTURE PENALTY)	0.765	0.855

RANKINE ENGINE DATA:

HEAT INPUT (BTU/HR) $(8.307 + 1.622) \times 10^6 = 9.929 \times 10^6$

WORK OUTPUT (BTU/HR) $(1.612 + 1.800) \times 10^6 = 3.412 \times 10^6$

HEAT REJECTED (BTU/HR) 6.517×10^6

FIGURE 23

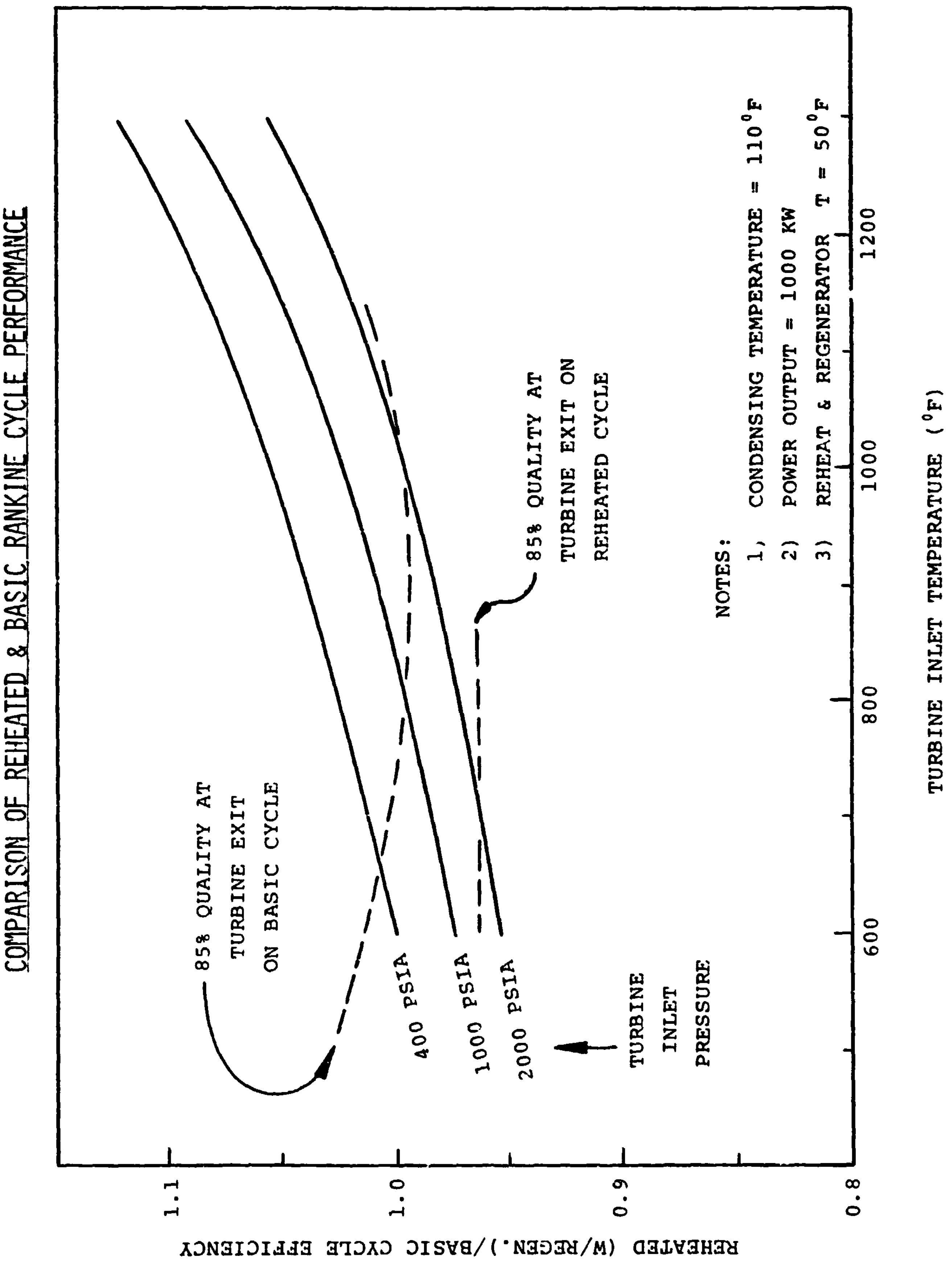
COMPARISON OF REHEATED & BASIC RANKINE CYCLE PERFORMANCE
85% QUALITY AT TURBINE EXIT ON BASIC CYCLE
400 PSIA
1000 PSIA
2000 PSIA
TURBINE INLET PRESSURE
85% QUALITY AT TURBINE EXIT ON REHEATED CYCLE
NOTES:
1, CONDENSING TEMPERATURE = 110°F
2) POWER OUTPUT = 1000 KW
3) REHEAT & REGENERATOR T = 50°F
600
800
1000
1200
TURBINE INLET TEMPERATURE (°F)
1.1
1.0
0.9
0.8
REHEATED (W/REGEN.)/BASIC CYCLE EFFICIENCY

FIGURE 24

STEAM RANKINE CYCLE

WITH FEEDWATER HEATING

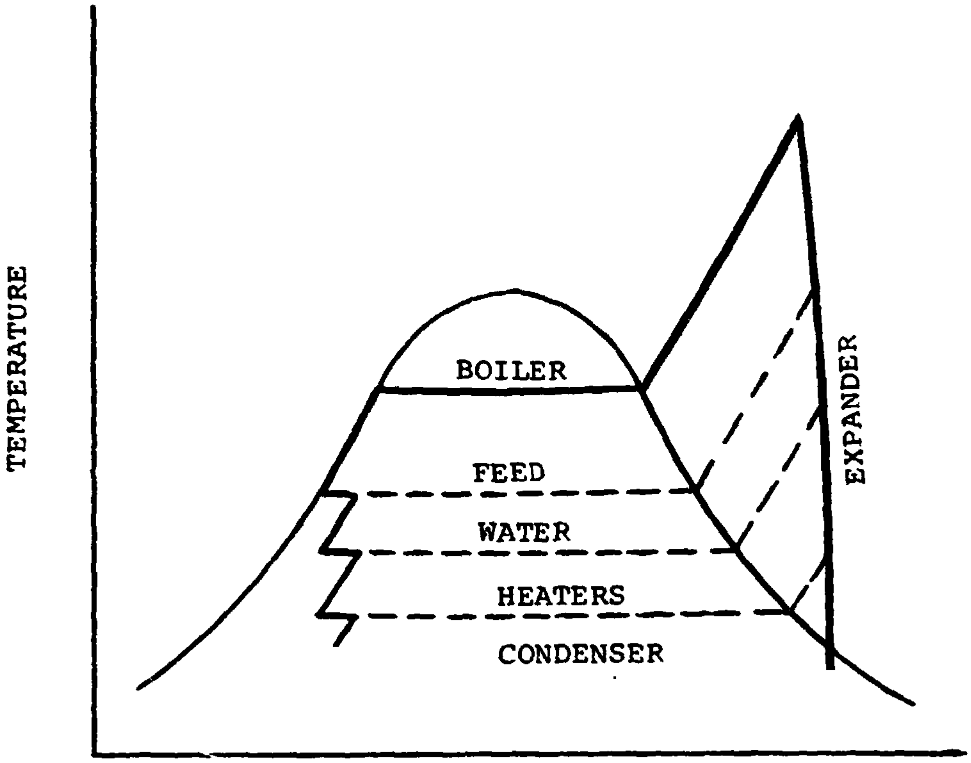
TEMPERATURE
BOILER
FEED
WATER
HEATERS
CONDENSER
EXPANDER
ENTROPY

FIGURE 25

STEAM RANKINE ENGINE WITH FEEDWATER HEATING

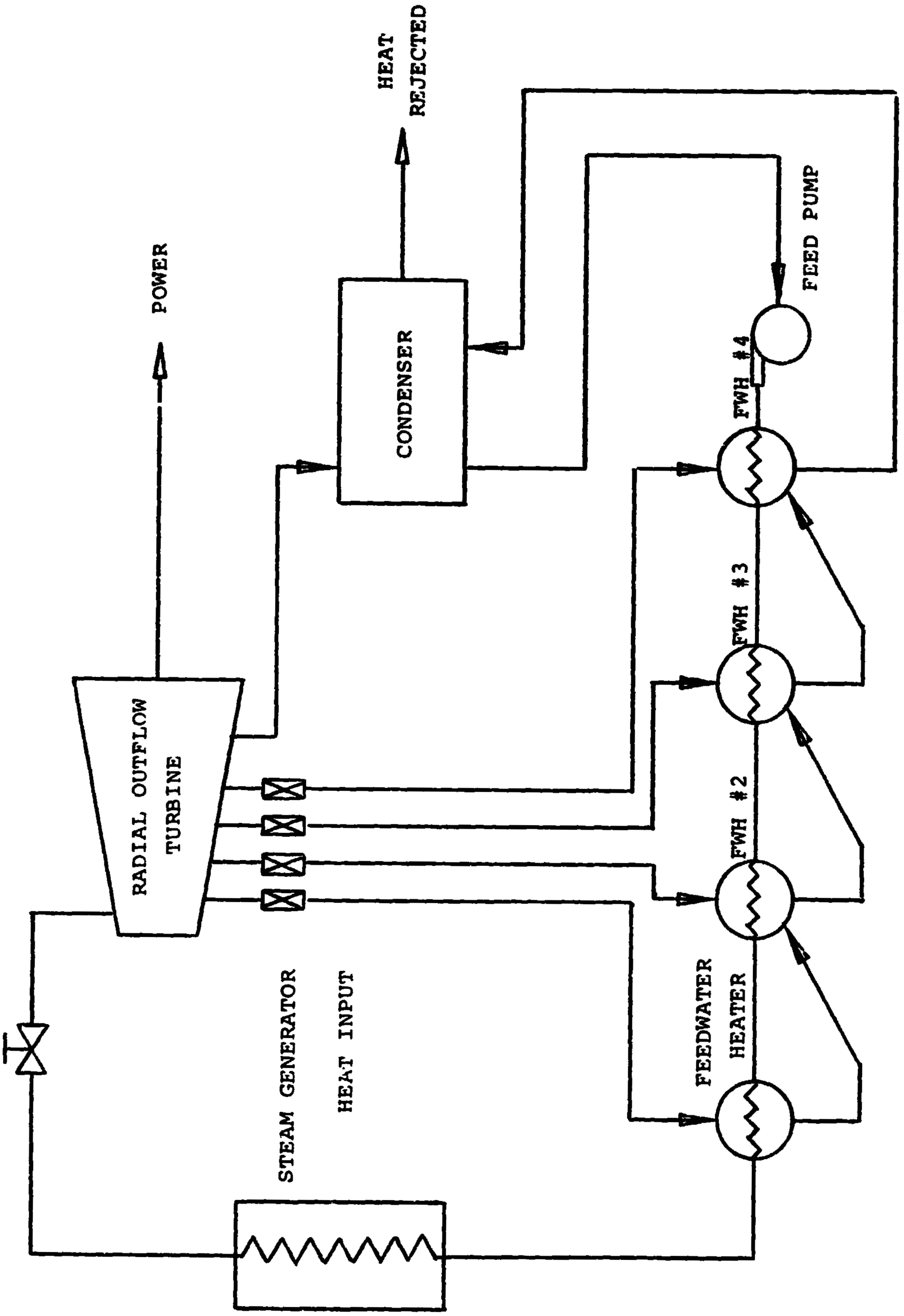
POWER
HEAT REJECTED
CONDENSER
FEED PUMP
RADIAL OUTFLOW TURBINE
FWH #4
FWH #3
FWH #2
FEEDWATER HEATER
STEAM GENERATOR
HEAT INPUT

FIGURE 26

FEEDWATER HEATING STEAM RANKINE CYCLE CALCULATION SHEET

TURBINE SPECIFICATIONS:

INLET: TEMPERATURE (°F) 1000 ENTHALPY (BTU/LB) 1505.4

PRESSURE (PSIA) 1000 ENTROPY (BTU/LB-°R) 1.6530

EXIT: PRESSURE (PSIA) 1.275 ENTHALPY (BTU/LB) 936.0

{CONDENSING TEMPERATURE (°F) 110 }

POWER OUTPUT (HP) 1341 (KW) 1000

SHAFT SPEED (RPM) 12,000 INLET MASS FLOW (LB/HR) 8260

ACTUAL EXIT: ENTHALPY (BTU/LB) 1012.9 QUALITY 0.906

SPECIFIC VOLUME (FT^3/LB) 240.7

MASS FLOW RATE (LB/HR) 6080

SPOUTING VELOCITY (FT/SEC) 1126

REYNOLDS NO. LAST STAGE 1.073 X 10^6

STAGE EFFICIENCY 0.940

EFFICIENCY (INCL. MOISTURE PENALTY) 0.865

FEEDWATER HEATER DATA:

NO.	PRESS.	LIQUID Δh	VAPOR Δh	MASS FLOW	TURBINE POWER OUTPUT
1	400	116.2	1105.7	865	0.599 X 10^6
2	110	86.4	1080.9	587	0.837 X 10^6
3	30	70.0	1042.9	454	0.742 X 10^6
4	7.5	49.8	1007.0	274	0.674 X 10^6
					0.560 X 10^6

RANKINE ENGINE DATA:

HEAT INPUT (BTU/HR) 9.106 X 10^6

WORK OUTPUT (BTU/HR) 3.412 X 10^6

HEAT REJECTED (BTU/HR) 5.694 X 10^6

ENGINE EFFICIENCY 0.375

FIGURE 27

ACTUAL TURBINE EXPANSION WITH EXTRACTION FOR FEEDWATER HEATING

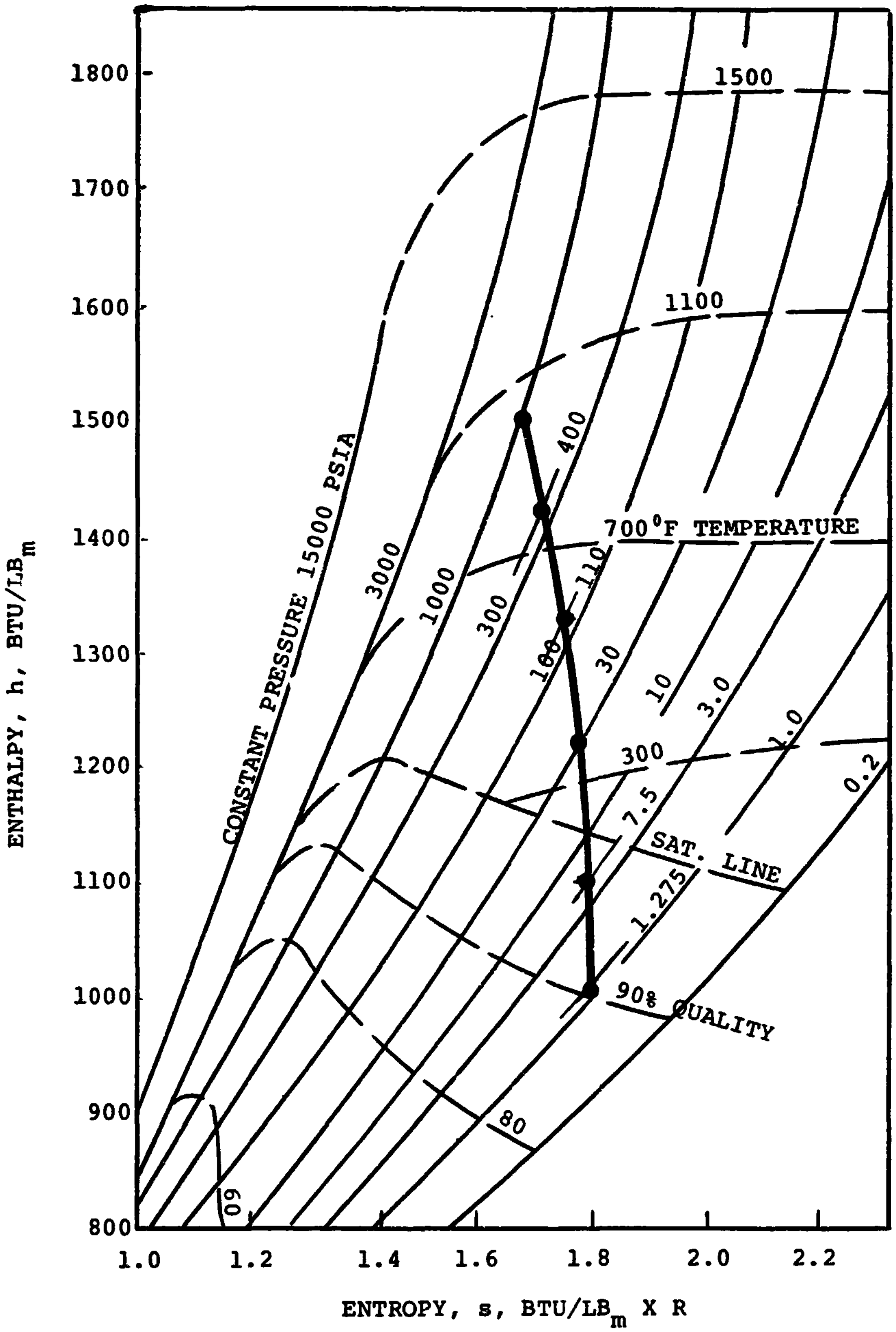

FIGURE 28

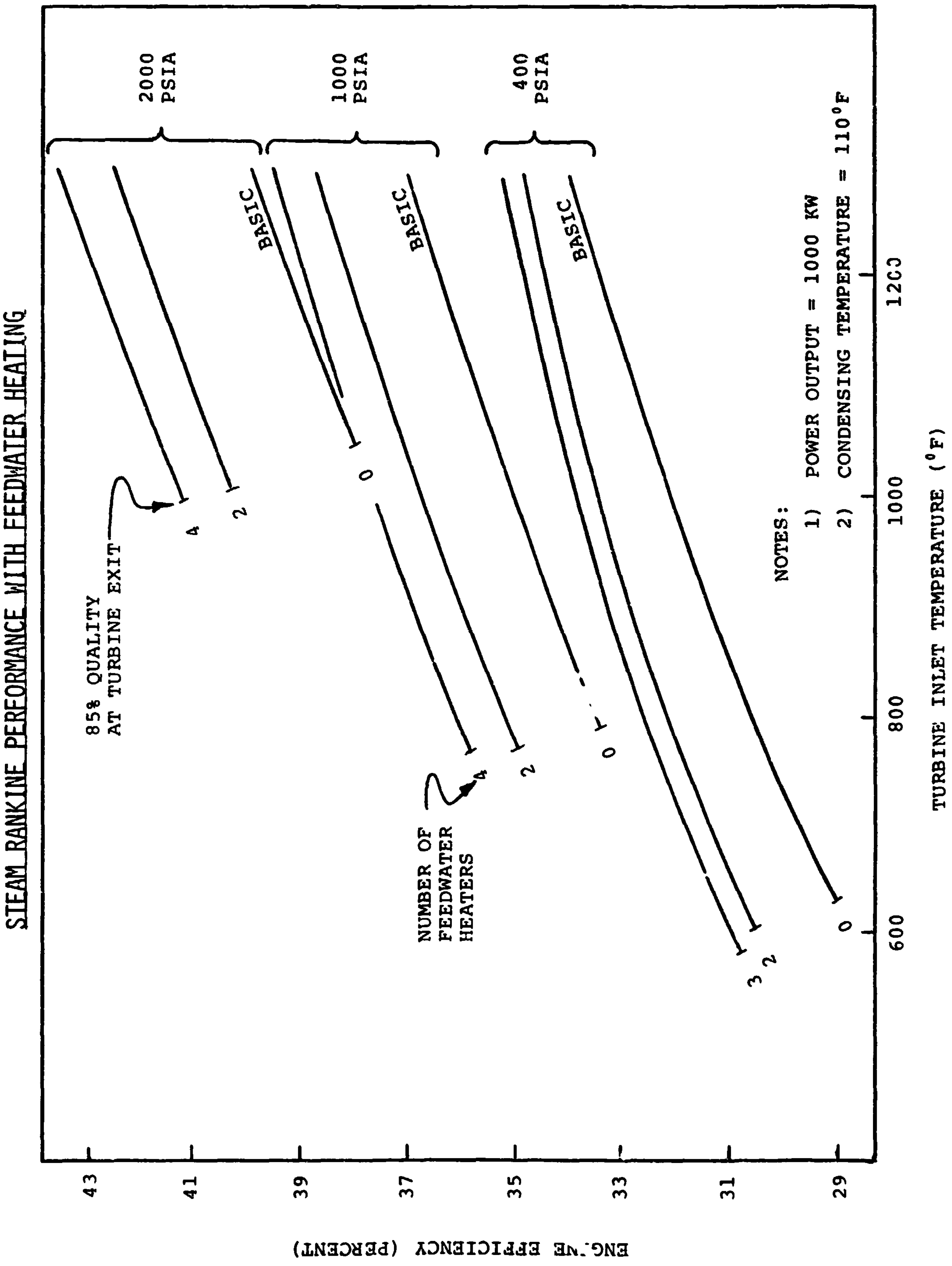
STEAM RANKINE PERFORMANCE WITH FEEDWATER HEATING
2000 PSIA
1000 PSIA
400 PSIA
BASIC
BASIC
BASIC
85% QUALITY AT TURBINE EXIT
NUMBER OF FEEDWATER HEATERS
4
2
0
4
2
0
3
2
0
NOTES:
1) POWER OUTPUT = 1000 KW
2) CONDENSING TEMPERATURE = 110°F
600
800
1000
1200
TURBINE INLET TEMPERATURE (°F)
43
41
39
37
35
33
31
29
ENGINE EFFICIENCY (PERCENT)

FIGURE 29

TURBINE FAMILY CONCEPT

DEFINITION

Beginning with a 5 MW ROF turbine design, power output is decreased until efficiency is reduced by 3 percentage points. A new ROF turbine design is then computed based on a higher shaft speed.

STEAM RANKINE CYCLE SPECIFICATIONS:

Turbine Inlet Conditions:

Temperature: 1000°F

Pressure: 1000 PSIA

Condensing Temperature: 110°F

POWER OUTPUT (KW)	SHAFT SPEED (RPM)	ROF TURBINE EFFICIENCY	OPTIMIZED SHAFT SPEED (RPM)	OPTIMIZED ROF TURBINE EFFICIENCY
5,000	5,000	0.880	-	-
2,800	5,000	0.850	7,150	0.878
1,570	7,150	0.848	9,700	0.872
880	9,700	0.842	12,720	0.864
500	12,720	0.834	16,210	0.855
285	16,210	0.825	20,300	0.844
160	20,300	0.814	25,280	0.833

GEARBOX AND GENERATOR EFFICIENCY VS. POWER OUTPUT

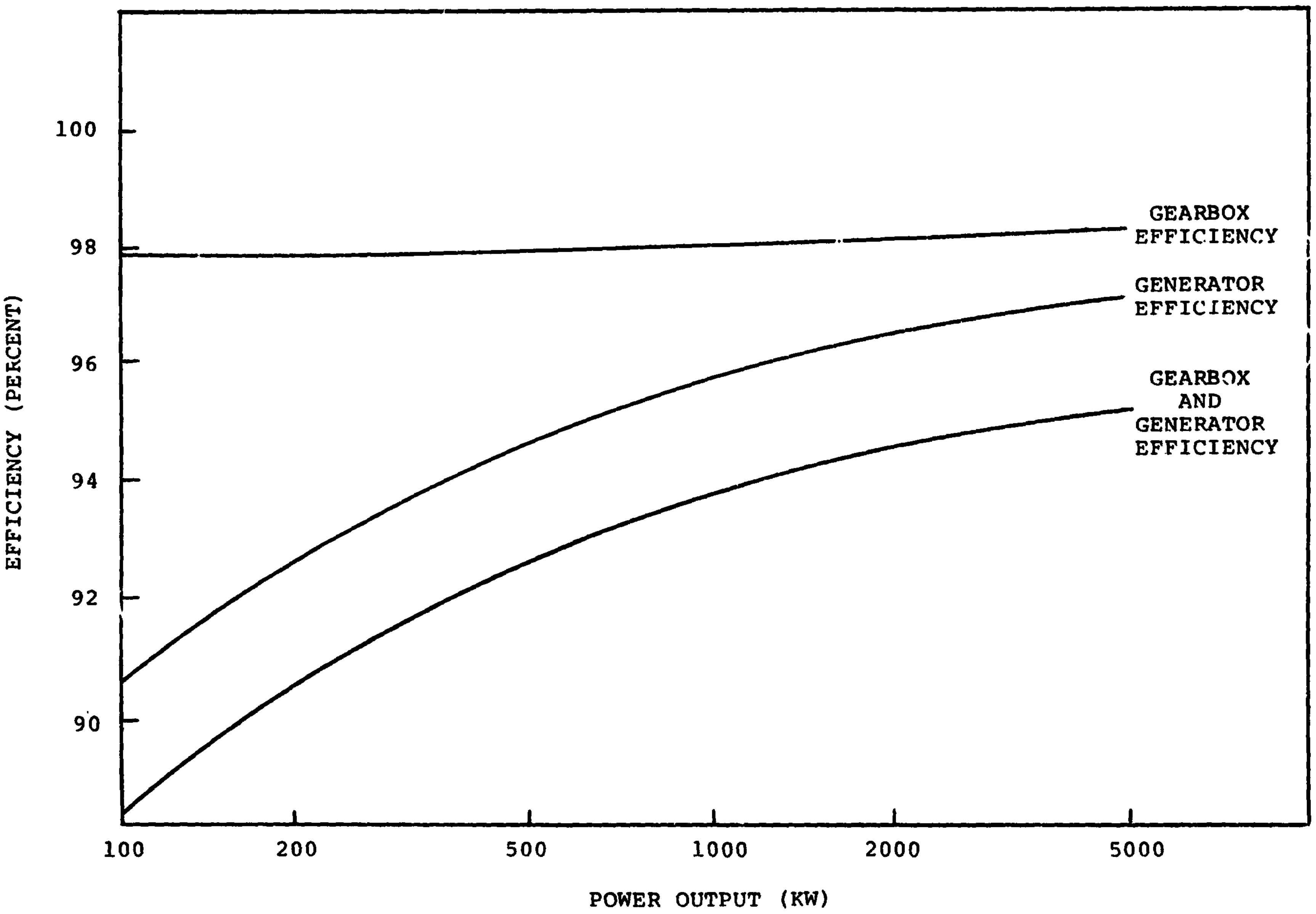

FIGURE 30

FIGURE 31

STEAM RANKINE ENGINE EFFICIENCY CALCULATION SHEET

TURBINE SPECIFICATIONS:

INLET TEMP. (°F) 1000 EXIT PRESS. (PSIA) 1.275

PRESS. (PSIA) 1000 COND. TEMP. (°F) 110

POWER OUTPUT (HP) 1341 (KW) 1000

SHAFT SPEED (RPM) 12,000

EFFICIENCY 0.869

RANKINE INGINE DATA:

HEAT INPUT (BTU/HR) 9.83×10^6

WORK OUTPUT (BTU/HR) 3.41×10^6

HEAT REJECTED (BTU/HR) 6.42×10^6

CYCLE EFFICIENCY 0.347

GEARBOX EFFICIENCY 0.980

GENERATOR EFFICIENCY 0.955

FEED PUMP POWER (KW) 8.44 (0.992)

CONDENSER POWER:

AIR-COOLED (KW) 36.59 (0.963)

WATER-COOLED (KW) 12.0 (0.988)

PCS AUXILIARY POWER (KW) 5 (0.995)

(LUBE SUPPLY, INSTRUMENTATIONS, CONTROLS)

OVERALL ENGINE EFFICIENCY: 0.309 (air-cooled)

0.317 (water-cooled)

FIGURE 32

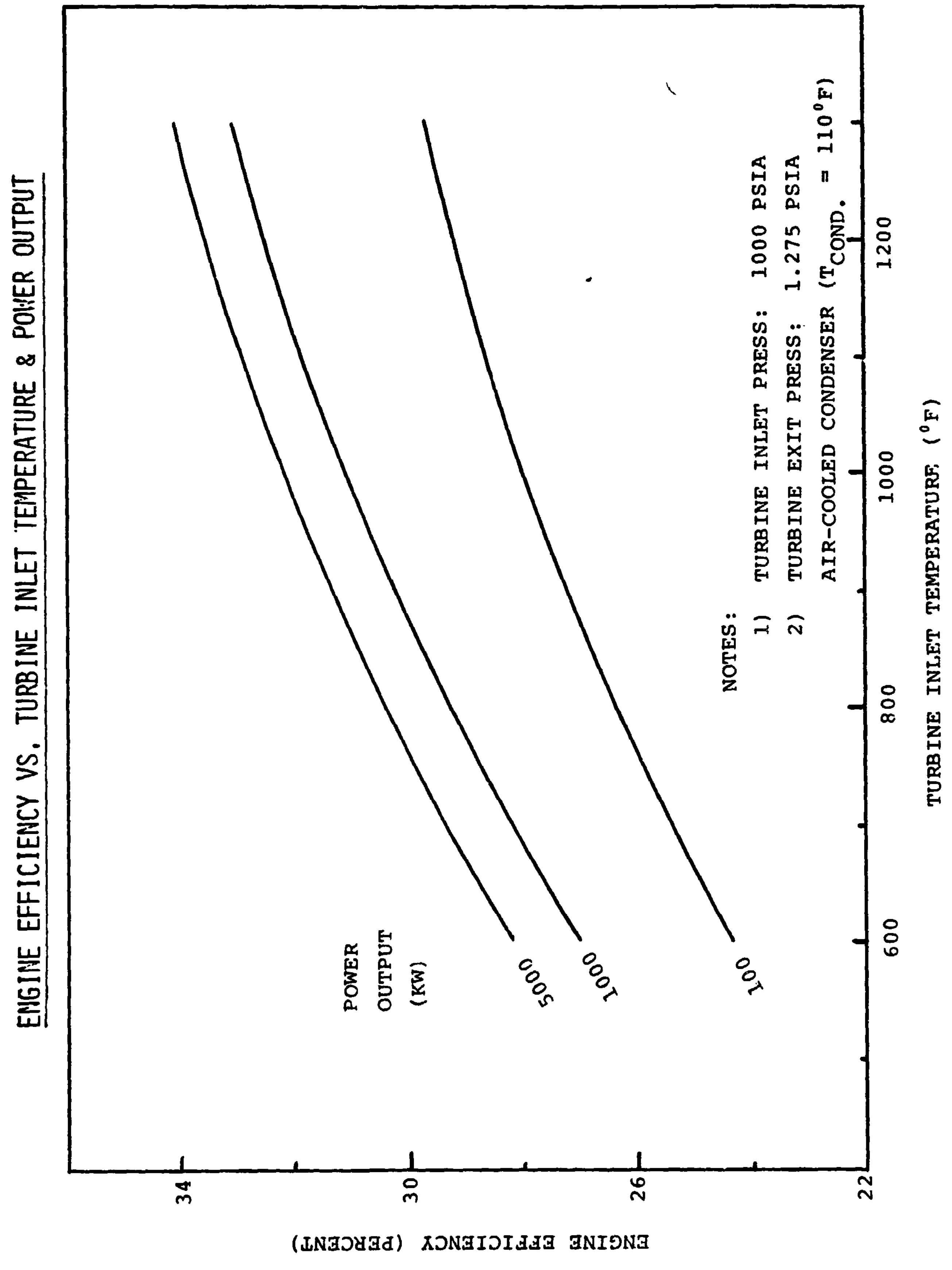
ENGINE EFFICIENCY VS. TURBINE INLET TEMPERATURE & POWER OUTPUT

FIGURE 33

ENGINE EFFICIENCY VS. TURBINE INLET TEMPERATURE & POWER OUTPUT

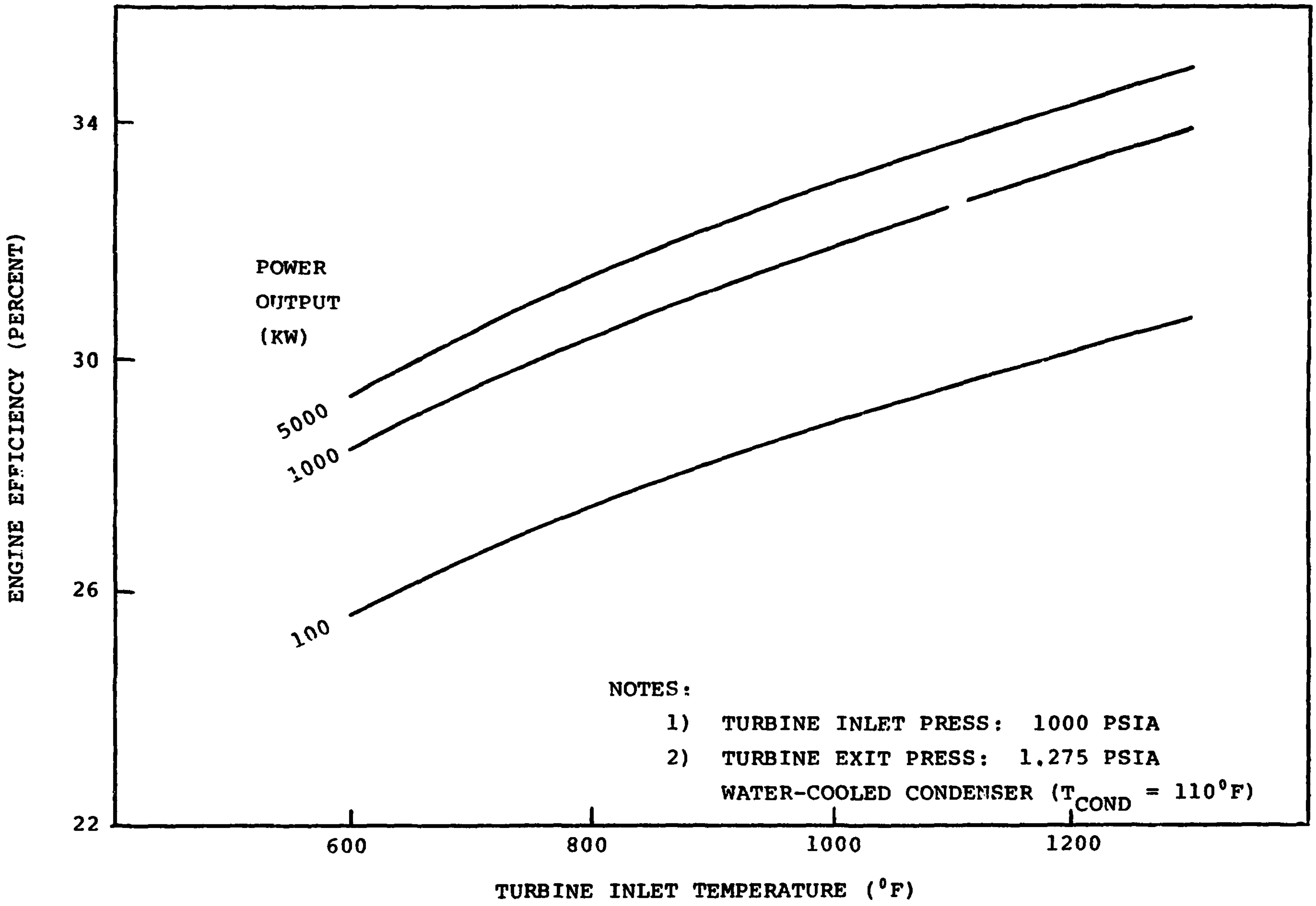

NOTES:

1) TURBINE INLET PRESS: 1000 PSIA
2) TURBINE EXIT PRESS: 1.275 PSIA

WATER-COOLED CONDENSER (T_{COND} = 110°F)

FIGURE 34

GEARBOX PART LOAD PERFORMANCE

Gearbox losses are primarily a function of speed, not load. In a solar electric power application, speed is a constant. A loss curve for the gearbox can therefore be predicted based on fixed losses irrespective of load:

LOAD (PERCENT)	GEARBOX EFFICIENCY
25	0.902
50	0.941
75	0.954
100	0.980

GENERATOR PART LOAD PERFORMANCE

Generator off-design efficiency is taken to be defined by commercial data:

LOAD (PERCENT)	GENERATOR EFFICIENCY	
25	0.920	0.839
50	0.952	0.905
75	0.957	0.911
100	0.955	0.908
	(1000 KW)	(100 KW)

Low load generator efficiency falls off more quickly in lower power units as evidenced in the above chart.

TURBINE PART LOAD PERFORMANCE

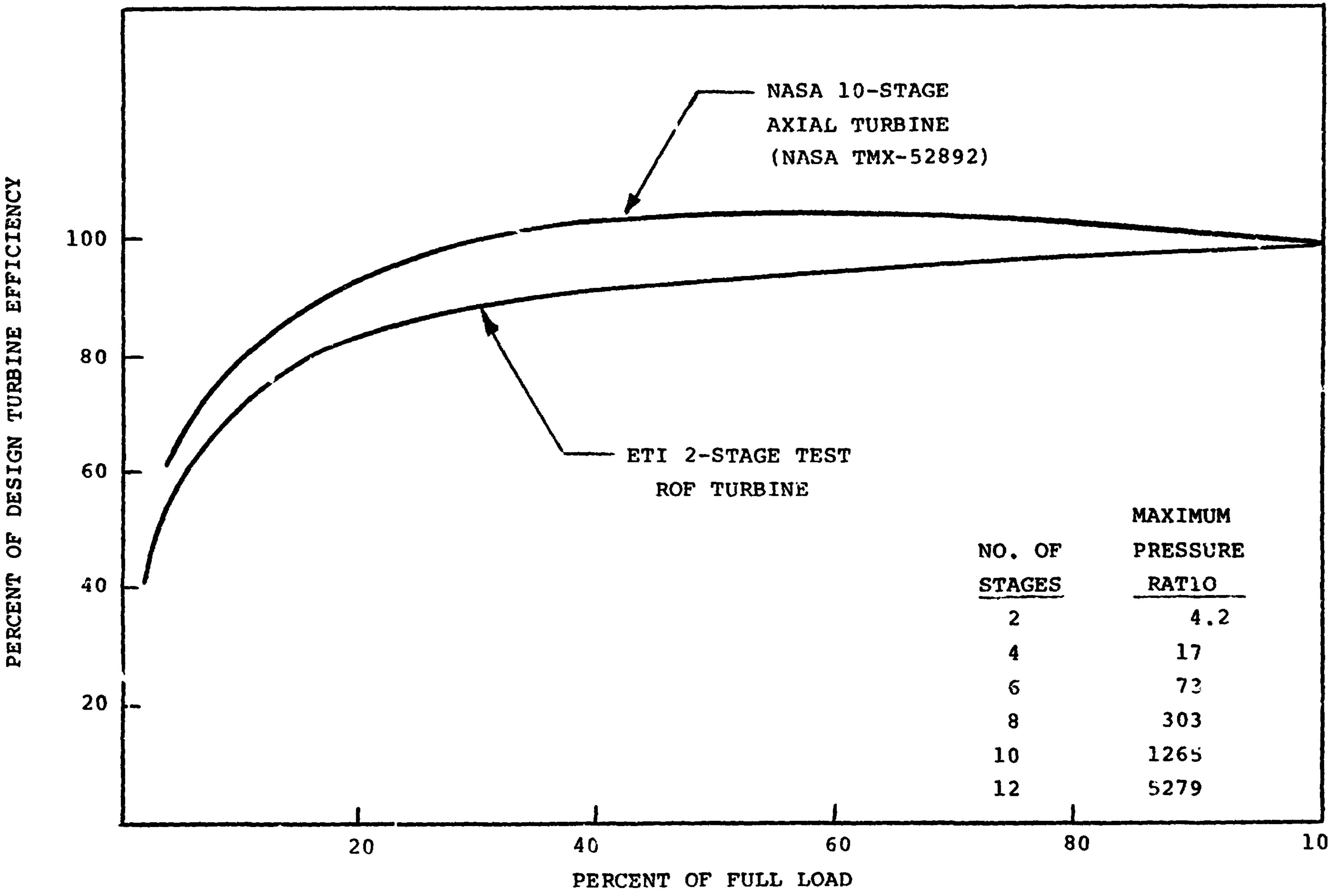

NO. OF STAGES	MAXIMUM PRESSURE RATIO
2	4.2
4	17
6	73
8	303
10	1265
12	5279

FIGURE 35

RANKINE ENGINE PART LOAD PERFORMANCE

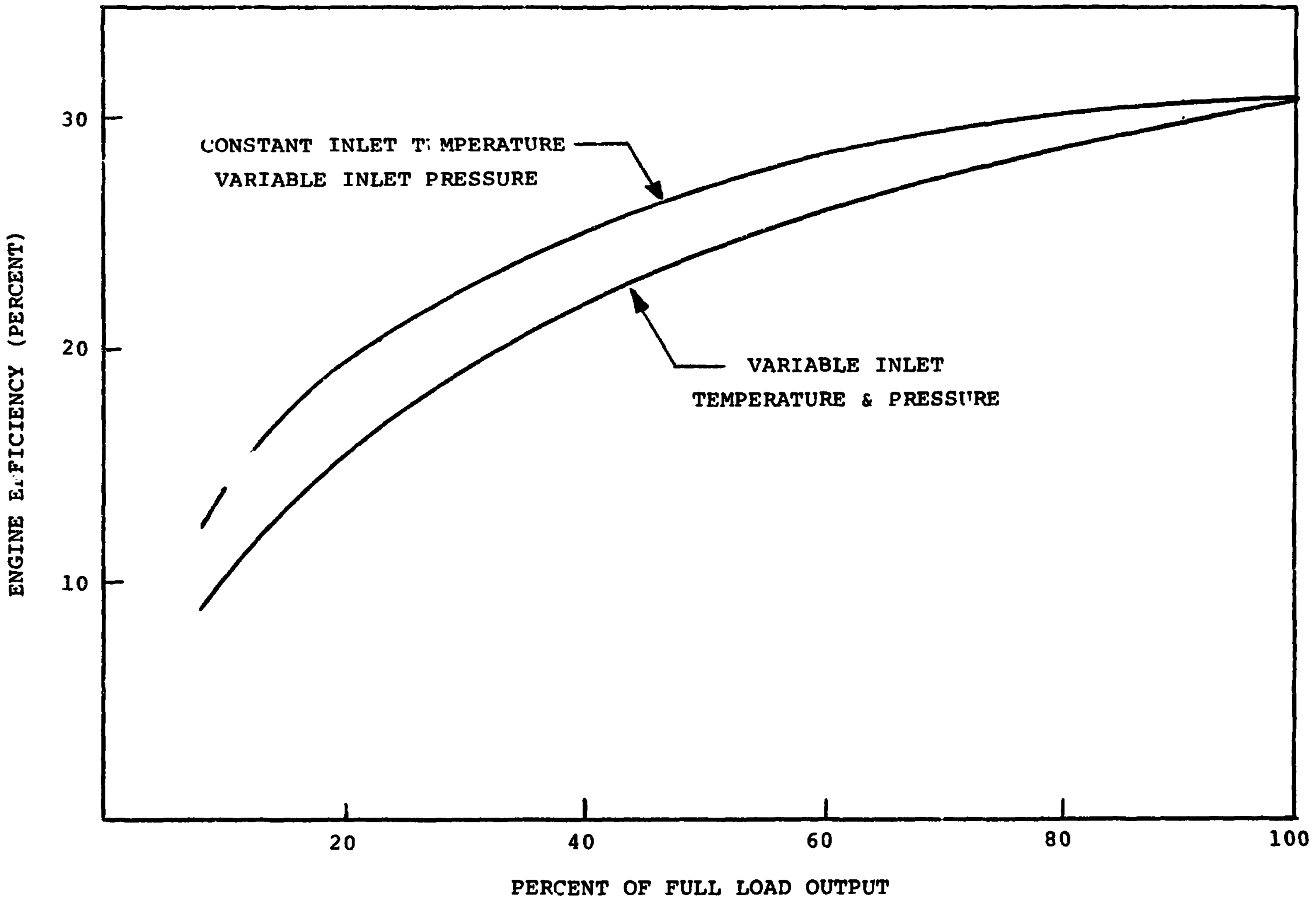

FIGURE 36

FIGURE 37

STEAM RANKINE ENGINE PART LOAD PERFORMANCE VS. POWER OUTPUT

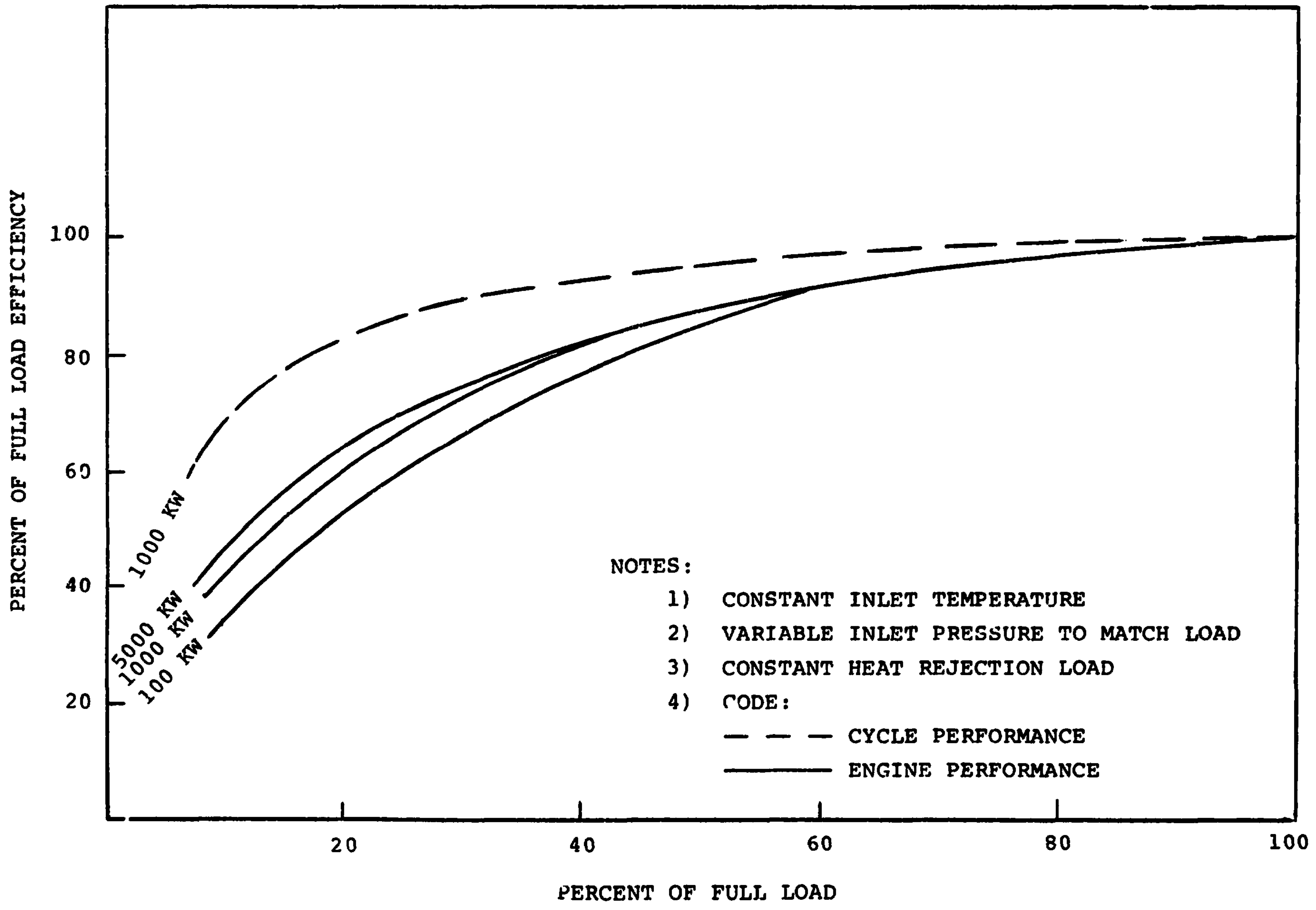

FIGURE 38

POWER CONVERSION SUBSYSTEM AND PLANT PERFORMANCE VS. LOAD

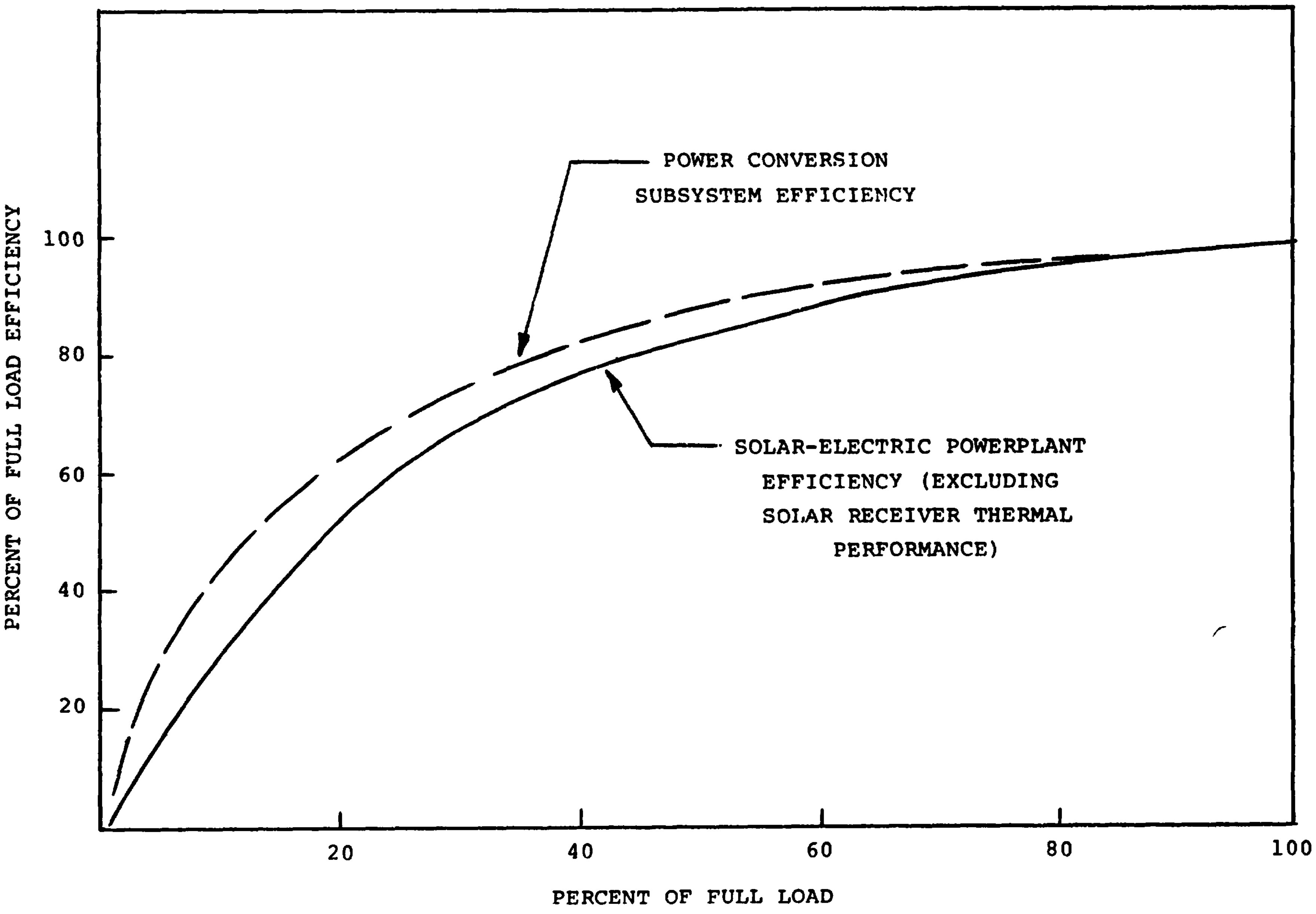

FIGURE 39

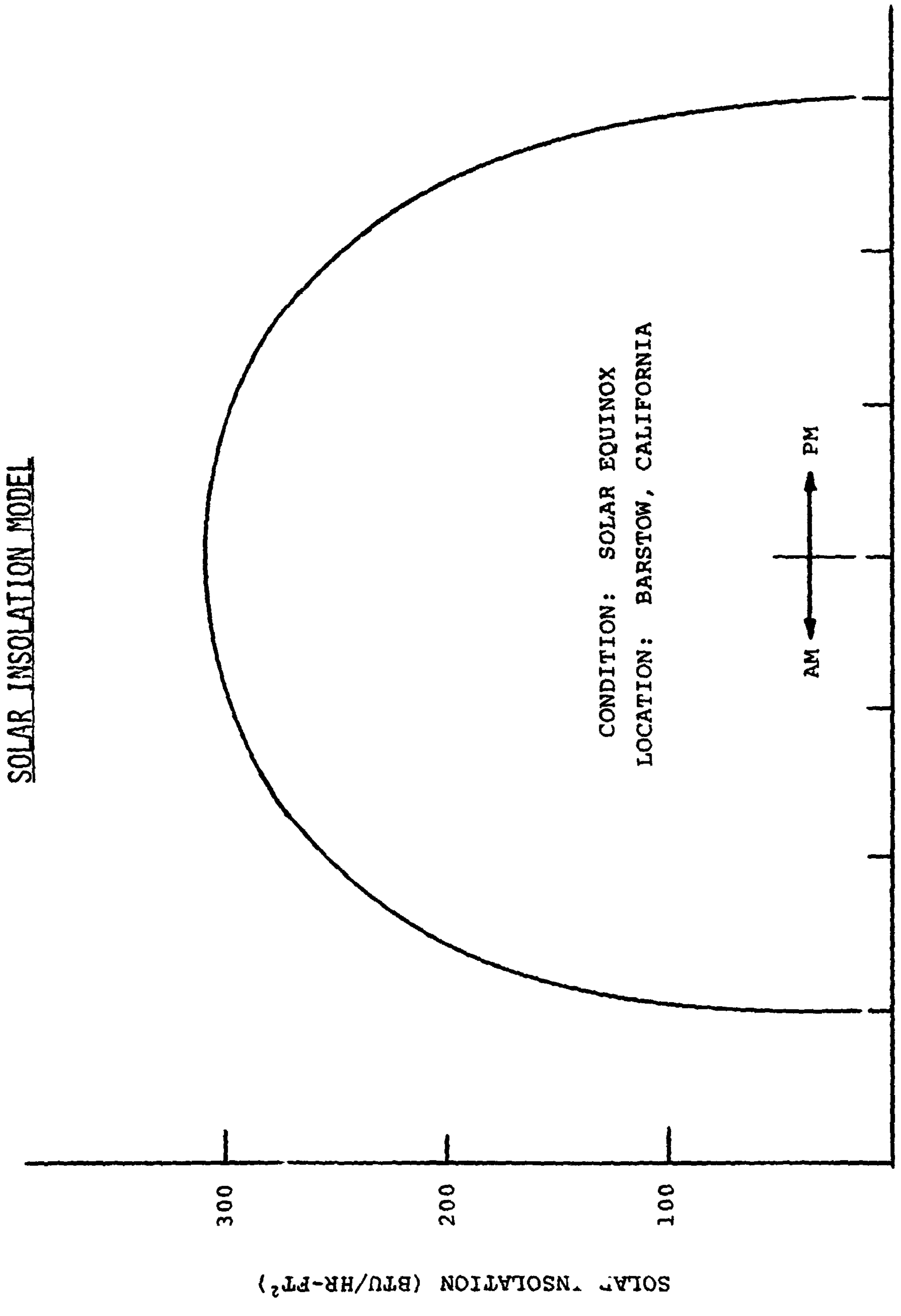
SOLAR INSOLATION MODEL
CONDITION: SOLAR EQUINOX
LOCATION: BARSTOW, CALIFORNIA
AM
PM
300
200
100
6
8
10
12
2
4
6
TIME OF DAY
SOLAR INSOLATION (BTU/HR-FT^2)

REFERENCES

1. Turbine Design and Application. A. Glassman, NASA Lewis Research Center. NASA SP-290. 1972.

2. Basic Investigation of Turbine Erosion Phenomena. W. D. Pouchot et al, Westinghouse Electric Corporation. NASA CR-1830. November 1971.

3. Foundations of a Theory of the Wet - Steam Turbine. G. Gyarmathy. AD-489-324. August 1966.

4. Phase I of the First Small Power System Experiment - Second Quarterly Technical Status Report. R. J. Holl and R. P. Dawson, McDonnell Douglas Astronautics Company. January 1979.